University of South Bohemia in České Budějovice
Faculty of science

Mechanism of photoprotection in photosynthetic proteins

Master thesis

Bc. Eliška Trsková, BSc.

Supervisor: Mgr. Radek Kaňa, PhD.

České Budějovice 2015

Diploma thesis:

Trsková E., 2015: Mechanism of photoprotection in photosynthetic proteins, Mgr. Thesis, in English – 57 p, Centre Algatech, Institute of Microbiology, Academy of Sciences of the Czech republic, The University of South Bohemia, České Budějovice, Czech republic

Abstract

Nonphotochemical quenching is an important protective mechanism of photosynthetic proteins against excessive irradiation. In this work, isolation of native light harvesting antennae from alga *Chromera velia* was optimized using methods of sucrose density centrifugation, isoelectric focusing, ion exchange chromatography and gel electrophoresis. Moreover, the ability of light harvesting antennae to trigger nonphotochemical quenching was studied *in vivo* and *in vitro*.

Abstrakt

Nefotochemické zhášení je důležitým ochranným mechanismem fotosyntetických proteinů při vysoké intenzitě ozáření. V této práci byla optimalizována izolace nativních světlosběrných antén z řasy *Chromera velia* za využití metod centrifugace na sacharózovém gradientu, izoelektrické fokusace, iontově výměnné chromatografie a gelové elektroforézy. Dále byla studována schopnost světlosběrných antén indukovat nefotochemické zhášení *in vivo* a *in vitro*.

Granty:

The work has been financially supported by the Czech Science Foundation (project GAČR, P501-12-0304) and by Ministry of Education, Youth and Sport - project ALGAMAN (CZ.1.07/2.3.00/20.0203). Centre of ALGATECH was financed by institutional project ALGATECH Plus (MSMT LO1416).

I hereby declare that, in accordance with Article 47b of Act No. 111/1998 in the valid working, I agree with the publication of my diploma thesis, in full to be kept in the Faculty of Science archive, in electronic form in publicly accessible part of the STAG database operated by the University of South Bohemia in České Budějovice accessible through its web pages.

Further, I agree to the electronic publication of the comments of my supervisor in accordance with aforementioned Act No. 111/1998. I also agree to the comparison of the text of my bachelor thesis with the Theses.cz thesis database operated by the National Registry of University Theses and plagiarism detection system.

Klec, 20.04.2015

……

Eliška Trsková

Acknowledgement

I would like to thank to Mgr. Radek Kaňa, PhD., for supervising of my theses and for his crazy funny laughing which made me feel relaxed and which made my mood better after bad experiments.

My big thanks go to Ing. Roman Sobotka, PhD., who explained to me all the mysterious things about isolation of *C. velia* proteins and who spent so much time with me and my work.

I would like to thank to Mgr. Eva Žišková, who helped me so much during practical work and who was always there if I needed support, help with visual style or something sweet to eat when my cultures died from unknown reasons.

I would also like to thank to all the members of Alexander Ruban lab in London, especially to Dr. Erica Belgio, who made my stay there so nice and full of amazing scientific experiences.

To all members of the centre Algatech I would like to thank for creating friendly atmosphere.

Last but not least I would like to thank to my family, boyfriend and friends for being patient and supportive all the time, especially when writing the diploma thesis.

Table of contents

List of abbreviation

ATP = Adenosine triphosphate

β-DDM, DDM = n-Dodecyl-β-D-maltoside

CLH complex = Chromera light harvesting complex

CN-PAGE = Clear native polyacrylamide gel electrophoresis

Dd-Dt cycle = diadinoxanthin - diatoxanthin cycle

$\mathbf{F_0}$ = Minimal fluorescence

FCPs = Fucoxanthin-chlorophyll a/c proteins

$\mathbf{F_M}$ = Maximum fluorescence in dark

$\mathbf{F_M'}$ = Maximal fluorescence during illumination

FPLC = Fast performance liquid chromatography

GPC = Gel permeation chromatography

HPLC = High performance liquid chromatography

IEC = Ion-exchange chromatography

IEF = Isoelectric focusing

LHC = Light harvesting complex

$\mathbf{NADP^+}$ = Nicotinamide adenine dinucleotide phosphate

NPQ = Nonphotochemical quenching

pI = Isoelectric point

PSI, PSII = Photosystem I, Photosystem II

qE = Energy dependent quenching

qI = Photoinhibitory quenching

qP = Photochemical quenching

qT = State-transition quenching

ROS = Reactive oxygen species

RuBisCO = Ribulose bisphosphate carboxylase/oxygenase

SDS-PAGE = Polyacrylamide gel electrophoresis with sodium dodecyl sulfate (SDS) as detergent

VDE = Violaxanthin de-epoxidase

ZE = Zeaxanthin epoxidase

1 Introduction

Photosynthesis is a complex chemical process in which light energy is converted into the energy of organic compounds. The mechanism relies on efficient transfer of light energy from light harvesting antennae into the reaction centers. Plants are able to convert approximately 500 trillion kg of carbon dioxide to carbohydrate each year (Karp, 2010), from this reason, the process of photosynthesis has become an object of study for possible production of bio fuels etc. Consequently, a research concentrated on all the mechanisms accompanying photosynthesis and subsequent improvement of the photosynthetic efficiency is nowadays a very important and supported scientific field.

One of the mechanisms controlling the excess energy in photosynthetic membrane under high light illumination is nonphotochemical quenching (NPQ). Harmful excess energy is dissipated safely as heat in this protective mechanism. Although the process of NPQ has been intensively studied recently, the exact mechanism is still not completely clear in higher plants and its understanding is even worse concerning mosses and algae.

The first aim of this master thesis was to select a proper photosynthetic strain useful for isolation of native pigment-protein complexes. A unicellular alga *Chromera velia* was chosen as a main model organism of the study. This species forms an evolutionary link between non-photosynthetic apicomplexan parasites and phototrophic algae. Moreover it can be easily grown in lab conditions. From these reasons *C. velia* is currently intensively studied around a world among laboratories interested in genetics, photosynthesis and also parasitism.

The second task was to optimize the biochemical methods for isolation of native light harvesting antennae from the thylakoid membrane. For this purpose, different techniques of protein isolation were tested – sucrose density gradient centrifugation, IsoElectric Focusing (IEF) and Ion Exchange Chromatography (IEC).

The third objective of the thesis was a biochemical characterization of the previously isolated light-harvesting antennae. In this step, following techniques were employed in order to get the information about pigment-protein composition: High Performance Liquid Chromatography (HPLC), native gel electrophoresis, and Sodium Dodecyl Sulfate – Polyacrylamide Gel Electrophoresis (SDS-PAGE). Moreover the pigment-protein complexes were tested by means of absorption and low temperature spectroscopy to prove that antennae proteins are intact and suitable for subsequent measurements and storage.

The last aim of the project was to study nonphotochemical quenching in native cells and in isolated pigment-protein complexes using fluorescence techniques. The NPQ measurements *in vivo* were performed with *C. velia* cells and the effect of proton-gradient uncoupler (ammonium chloride) addition at different period of irradiation was tested. The NPQ measurements *in vitro* were performed in a reaction assay containing isolated antennae complexes. In order to test the sensitivity of NPQ to protein aggregation and to low pH, reaction assay was diluted and then acidified by adding hydrochloric acid. The reversibility of the process was subsequently proved by adding n-Dodecyl-β-D-maltoside (β-DDM) into the reaction.

2 Photosynthesis

2.1 Overview

Sunlight is a necessary source of energy for phototrophic organisms. This light energy is used in a bioenergetical process called photosynthesis. In this mechanism, the Sun light provides energy for driving reactions producing organic substances from carbon dioxide (CO_2) and water (H_2O). Whereas phototrophic organisms are able to produce organic substances during this process, heterotrophic organisms require the supply of these compounds from their environment. Moreover molecular oxygen (O_2), which is necessary for all higher organisms, is formed as a byproduct of the photosynthetic reactions.

A simplified model of photosynthesis is the following: six molecules of CO_2 are converted into one molecule of sugar (hexose). Water provides necessary electrons for CO_2 reduction process when it is enzymatically split by light. A schematic reaction of the whole process of photosynthesis is the following.

$6\ CO_2 + 12H_2O \rightarrow C_6H_{12}O_6 + 6H_2O + 6O_2$

It is important to note that in the preceding scheme, each molecule of oxygen is not derived from CO_2 as it was originally estimated but from the water splitting reaction.

The mechanism of photosynthesis is historically divided into two series of reactions acting simultaneously: light-dependent reactions and light-independent reactions, i.e. dark reactions. During the first part, water molecules are split into oxygen atoms, protons and electrons, which are then used for re-reduction of pigments in reaction centers of photosystems. The photosystems are excited by light to a state, when pigments in reaction centers reach energy level sufficient for reducing plastoquinon or $NADP^+$. The resulting reactions mediate the formation of reduced plastoquinon and $NADPH + H^+$, when the latter is used during CO_2. The second product of the light reaction required for CO_2 fixation is adenosine triphosphate (ATP). The whole dark part of photosynthesis is called Calvin-Benson cycle and it requires appropriate enzymes to be present.

2.2 Light reactions

Eukaryotic photosynthetic organisms (green algae, higher plants) contain specialized organelles, chloroplasts. These organelles have appeared during secondary endosymbiosis together with other energetically important organelles – mitochondria. Therefore, they have their own genetic information found in the DNA structure of ring. The structure of plant

chloroplast is depicted in the Figure 1. It consists of two surrounding membranes, outer and inner one enclosing chloroplast interior called stroma. Stroma contains inner thylakoid membranes in a form of flattened membrane sacs that are stacked in grana. The granal thylakoids are connected by unstuck stromal thylakoids. Lumen is the interior of both, granal and stromal thylakoid. The enzymes located in thylakoid membrane are necessary for catalyzing the light reactions; dark reactions then take place in stroma.

Similarly to the respiratory chain, during the light reactions electrons are passing from one redox system to the next one in the so called electron transport chain. However, direction of this flow is different – in the respiratory chain, electrons flow from reduced $NADH+H^+$ to O_2 with the production of water and energy. The process is reversed in photosynthesis: water molecule provides electrons for "uphill" $NADP^+$ reduction requiring light energy from two photosystems, photosystem I and II (PSI and PSII, respectively). Photosystems are huge pigment-protein complexes that contain a lot of chlorophyll molecules together with other pigments including carotenoids.

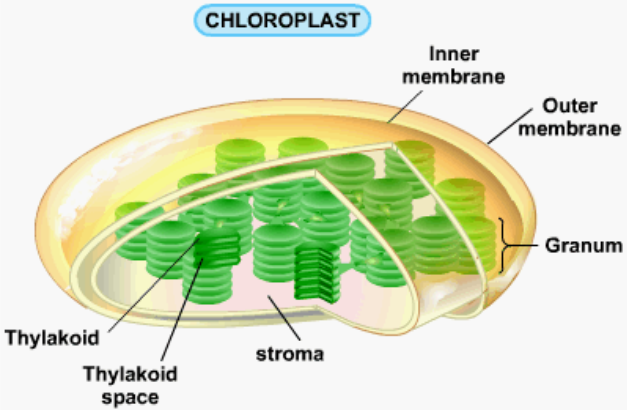

Figure 1: The structure of chloroplast (http://www.s-cool.co.uk/a-level/biology/cells-and-organelles/revise-it/organelles)

There is another very important player in photosynthetic electron transport chain, cytochrome b_6/f complex. It is integral membrane protein supercomplex with several co-factors including two cytochromes – cytochrome b563 and cytochrome f – and with other electron carriers. The function of cytochrome b_6/f complex is to transfer electrons from plastoquinol to plastocyanin and consequently from the reaction center of Photosystem II to Photosystem I, i.e. it functions as a proton pump (Koolman and Roehm, 2005).

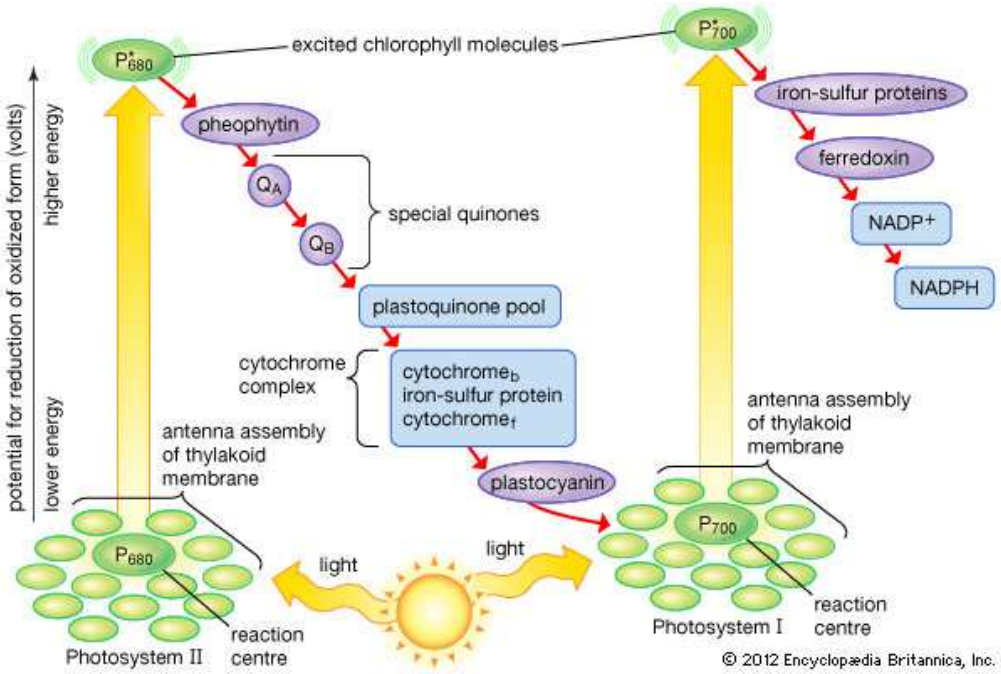

Figure 2: A simplified overview of the processes taking place during light-dependent reactions. P_{680} = Reaction centre of PSII, Q_A, Q_B= Plastoquinones P_{700}= reaction centre of PSI (http://www.britannica.com/EBchecked/media/3105/Flow-of-electrons-during-the-light-reaction-stage-of-photosynthesis)

PSII and cytochrome b_6/f transfer protons into thylakoid lumen and thus form the electrochemical gradient through thylakoid membrane. This gradient is then used for synthesis of ATP catalyzed by enzyme ATP synthase. A schematic overview of the light-dependent stage of photosynthesis is represented in Figure 2.

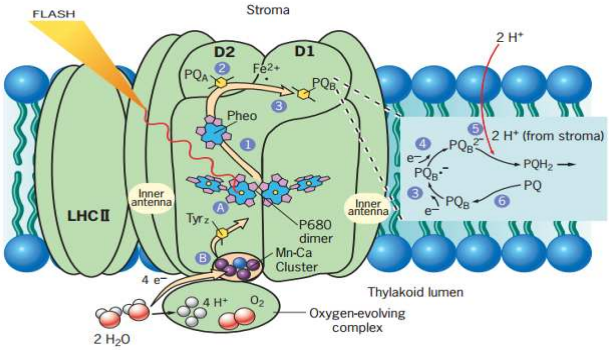

Figure 3: The structural organization of the Photosystem II together with the overview of the electron transport in PSII. PQ =Plastoquinone, D1, D2= polypeptides that form the heterodimeric reaction center core of PS II, LHC II = light harvesting complex II (Karp, 2010)

2.3 Photosystem II

Photosystem II (Figure 3) is the starting point of linear photosynthetic electron transport chain. PSII consists of many protein subunits that contain pigments molecules involved in light absorption and in excitation energy transfer. The most important co-factors of PSII are chlorophyll molecules in light harvesting antennae and in reaction

center P680 and two bound plastoquinones, Qa and QB. The structural organization of the photosystem II together with important co-factors is depicted in the Figure 3.

Electrons flow from water to plastoquinone and only about 1 % of the chlorophyll molecules are directly involved in charge separation taking place in reaction centers. The reason for this phenomenon is that the majority of the pigments (chlorophylls, carotenoids etc.) are components of the light harvesting antennae, where these pigment – protein complexes help to maximize the efficiency of photosynthesis and to transfer the absorbed energy to the reaction centers for further utilization (Buchel, 2015).

A simplified overview of the processes taking place in PSII is the following: Firstly, the chlorophyll reaction center is excited to higher energetic level with the use of excitation energy transferred from light-harvesting antennae. Charge separation in reaction centre forms electron that subsequently reduces pheophytin (modified chlorophyll without Mg^{2+}). The reaction center is re-reduced by an electron from the water splitting reaction mediated by oxygen evolving complex. The electron originated in charge separation flows from pheophytin to the quinone acceptors, Q_A and Q_B, where the semiquinone radical is formed. Afterwards Q_B undergoes reduction by second electron originated in the second charge separation event resulting in the hydroquinone form; that is immediately exchanged for oxidized plastoquinone from the plastoquinone pool. A further process of electron transport continues according to the scheme already explained in the light reactions chapter 2.2.

2.4 Dark reactions: Calvin-Benson cycle

Calvin-Benson cycle is a process involving chemical reactions leading to the synthesis of hexoses from CO_2. This reaction is catalyzed by the enzyme ribulose bisphosphate carboxylase/oxygenase – “RuBisCO”, which is the most abundant enzyme on our planet. This enzyme is able to convert ribulose 1,5-bisphosphate together with CO_2 and H_2O into the two molecules of 3-phosphoglycerate. These molecules are then converted into glyceraldehyde 3-phosphate through 1,3-bisphosphoglycerate and 3-phosphoglycerate.

As a result, twelve molecules of glyceraldehyde 3-phosphate are formed from six molecules of CO_2. Two of these synthesized molecules are utilized during a process of gluconeogenesis to produce glucose 6-phosphate. The remaining ten molecules of the intermediate (glyceraldehyde 3-phosphate) are used to regenerate six molecules of ribulose 1,5-bisphosphate, which are used in the cycle again.

It is important to note, that ATP is needed for the phosphorylation of 3-phosphoglycerate and ribulose 5-phosphate. Moreover the second product of the light

reaction - $NADPH+H^+$ - is consumed when reducing 1,3-bisphosphoglycerate to glyceraldehyde 3-phosphate.

2.5 Pigments

The first step of photochemical reactions is the absorption of light, which enables photosynthetic organisms to use the energy from light. It is important to note that formation of the energetically rich molecules (ATP, $NADPH+H^+$) during photosynthesis is a complex procedure which requires pigments. These compounds are coloured molecules due to their ability to absorb visible light.

Chlorophylls, for instance, appear green as they absorb blue and red part of visible spectrum, consequently only green light is transmitted. Due to evolution of special chlorophyll properties, these chromophores became major photosynthetic pigments. For instance, their excited lifetimes in dilute solutions can be up to three orders of magnitude longer than the rate of energy transfer, moreover their energy of first excited state is equivalent to the energy of almost six ATP molecules, which makes them possible to drive the processes ending with accumulation of ATP (Ruban, 2013).

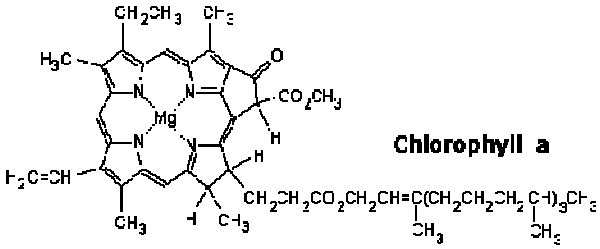

Figure 4: Structure of the chlorophyll a (http://www.food-info.net/uk/colour/chlorophyll.htm)

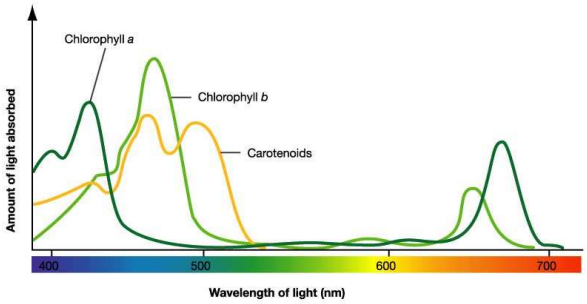

Figure 5: A typical absorption spectrum of chlorophylls and carotenoids. (http://www.ledgrowlightshq.co.uk/ chlorophyll-plant-pigments)

Chlorophyll molecule (Figure 4) consists of two parts – a porphyrin ring, which is responsible for light absorption, and a hydrophobic phytol chain, which helps to integrate chlorophyll into the photosynthetic membrane. Absorption spectrum of chlorophylls shows two regions in the visible light spectrum as you can see in Figure 5. The first one corresponds to the first excited state and it is found in the red part of the spectra. The second maximum is located in the blue region and it corresponds to the absorption into the second excited state. Chlorophylls are common light-harvesting pigments, however, photosynthetic organisms use also orange and red accessory pigments.

Xanthophylls (or oxygenated carotens) are commonly found in nature with versatile functions from powerful antioxidants, natural colorants to vitamin precursors. The most abundant plant antenna xanthophylls are lutein, neoxanthin, violaxanthin and zeaxanthin. Violaxanthin, carotenoid found also in *C. velia*, is a symmetrical molecule which is de-epoxidized to zeaxanthin in the photosynthetic membrane through the intermediate antheraxanthin. A summary absorption spectrum of carotenoids and chlorophylls is depicted in Figure 5.

2.6 Photosynthetic antennae

All photosynthetic organisms require light harvesting systems to improve absorption cross section of their photosystems and to widen the spectral range used for photosynthesis. Many different light harvesting systems evolved during evolution. These systems commonly contain chlorophylls and xanthophylls, but their complete pigment composition, number of protein subunits and also the interactions with photosystem reaction centers are different. The light harvesting function of antennae is enabled by pigments with high light harvesting properties (chlorophylls, carotenoids, etc.), binding pigments with relatively broad absorption bands and by extremely high pigment concentrations. There are three crucial properties of light harvesting antennae (Ruban, 2013): Absorption cross-section – which depends on the number of pigments and their ability to feed the reaction centers with excitation energy; Excitation energy lifetime – how long the energy is stored in the antennae complexes till it is delivered to the reaction centers; and Energy migration efficiency – which is influenced by positioning, mutual orientation and spectral properties of pigments.

We can distinguish between two major types of light harvesting antennae (see Figure 6): integral antennae composed of integral membrane proteins; and peripheral antennae that are associated with membrane and reaction centers through non covalent (usually electrostatic) interactions. Integral antennae can be further classified into three types: fused, core and accessory antennae. Fused antennae are integrated into the reaction center and they also share the same polypeptide – e.g. PSI reaction center of higher plants

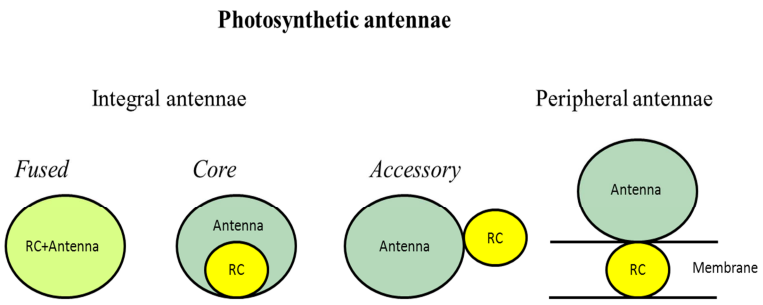

Figure 6: Classification of photosynthetic antennae (Ruban,

with two polypeptides that bind photochemically active reaction center chlorophyll together with large number of chlorophyll *a* molecules functioning solely as light harvesting pigments. Core antennae are also associated with reaction centers of photosystems; however they do not share the same polypeptides – e.g. antennae of PSII, CP43 and CP47 which bind only chlorophyll *a*. The last type of antennae are accessory antenna complexes composed of proteins that can be found in various localizations from the reaction center and which are arranged separately from it – e.g. major LHCII complex of PSII and LHCI complexes of PSI. The schematic overview of photosynthetic antennae is depicted in Figure 6.

The membrane intrinsic light harvesting proteins (Lhc) are found throughout majority of eukaryotic photosynthetic organisms (Wolfe et al., 1994). Proteins of this family have usually three membrane spanning α-helices that are connected by loops of different sizes. The overall structure of one representative of this group CP29 – one of the minor antenna proteins from PSII - is shown in Figure 7. However, the protein family contains also one or two helices proteins as well as four helices proteins – e.g. PsbS (Engelken et al., 2010). All Lhc are nuclear encoded proteins binding chlorophylls and carotenoids. Two helices (A and B) are homologous, possibly originated from gene duplication event (Green and Pichersky, 1994) and form a kind of cross. They also comprise conserved chlorophyll binding sites leading to symmetric location of chlorophylls around them. The space between helix C and the pair of helices A and B is full of pigments responsible also for 3D structure of the whole complex.

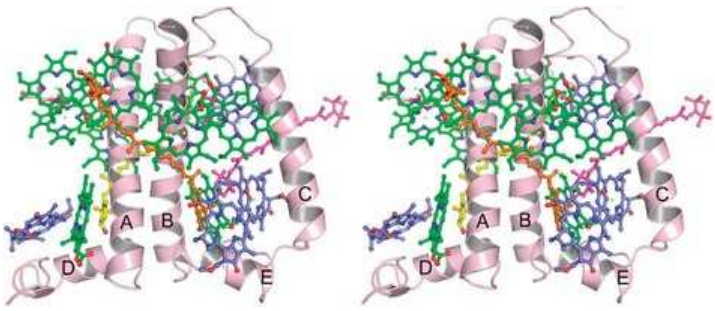

Figure 7: Stereo view of CP29 in parallel with the membrane plane. Helices A–E are labeled in the same way as they are in spinach LHCII. Chl phytol chains are not shown. Color explanation: Green = Chl a, blue = Chl b, yellow = Lut, orange = Vio, magenta = Neo, light pink = G3P (Pan et al., 2011)

The genes of the Lhc family are divided into two groups, one group coding for the Chl *a/b* binding proteins of green algae, mosses and higher plant and the second group coding for other Lhc sequences (Neilson and Durnford, 2010). The former group can be further divided into the two main branches: the *Lhca* genes coding for PSI antenna, and *Lhcb* genes coding for PSII antennae. The remaining group is subdivided into *Lhcf* (dinoflagellates), *Lhcr* (cryptophytes, dinoflagellates), *Lhcx* (some dinoflagellates) and *Lhcz* (cryptophytes). Haptophytes, brown algae and diatoms contain all types of former mentioned genes (see review Buchel, 2015). Phylogenetic relationships between light harvesting systems of different algal groups are depicted in Figure 8.

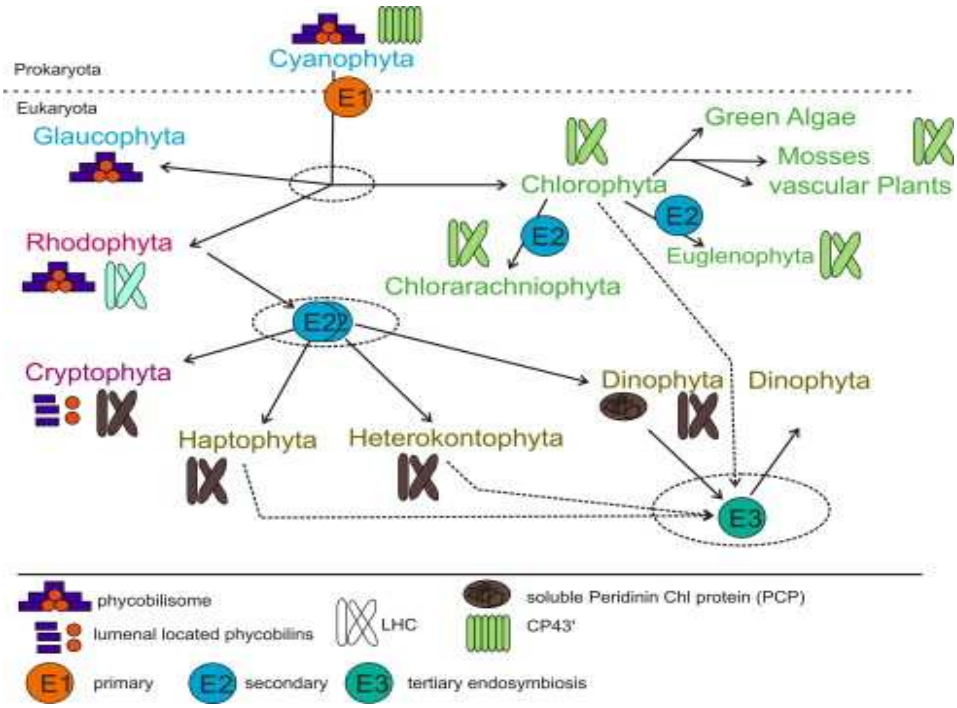

Figure 8: Overview of phylogenetic relationships between light harvesting systems of different algal groups. Circle = relationships under debate, dotted lines = possible routes for tertiary endosymbiosis (Buchel, 2015)

3 Nonphotochemical quenching

3.1 Introduction

Photosynthetic organisms are exposed to different light intensities during a day. These changes are either temporal (day cycle) or spatial (clouds shading the Sun etc.) and they can be very fast. Planktonic algae, for instance, are exposed to varying light conditions due to water mixing especially in a period of a few minutes (MacIntyre et al., 2000). Excessive light cannot be used in photosynthesis properly and it results in the formation of reactive oxygen species (ROS), which can be harmful or even fatal to the proteins in the photosynthetic machinery. Consequently, plants and algae had to evolve several protective mechanisms to survive and overcome periods of excessive light.

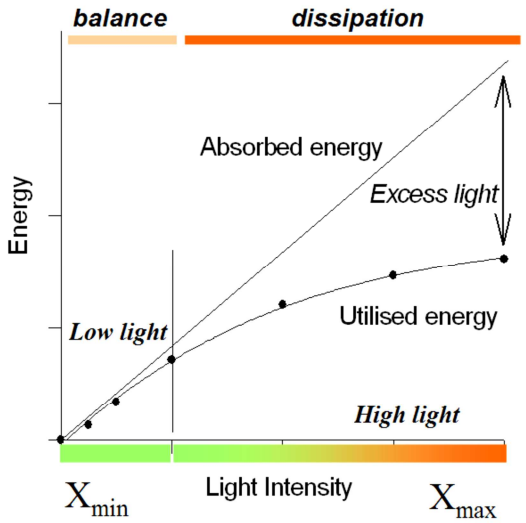

Figure 9: The energy workflow in dependence to light intensity (Ruban, 2013)

One of these mechanisms is called nonphotochemical quenching (NPQ) that can be characterized as a safe dissipation of excess energy in the form of heat (Horton et al., 1996), (Goss and Lepetit, 2014). A mechanism of NPQ can be studied by means of variable fluorescence methods, as NPQ value is reflected in the quenching of the chlorophyll a fluorescence. NPQ can be stimulated fast and that is why it is able to overcome sudden changes in light intensities. NPQ mechanism is still not completely understood but it consists of multiple processes. Figure 9 demonstrates energy workflow dependence on light intensity.

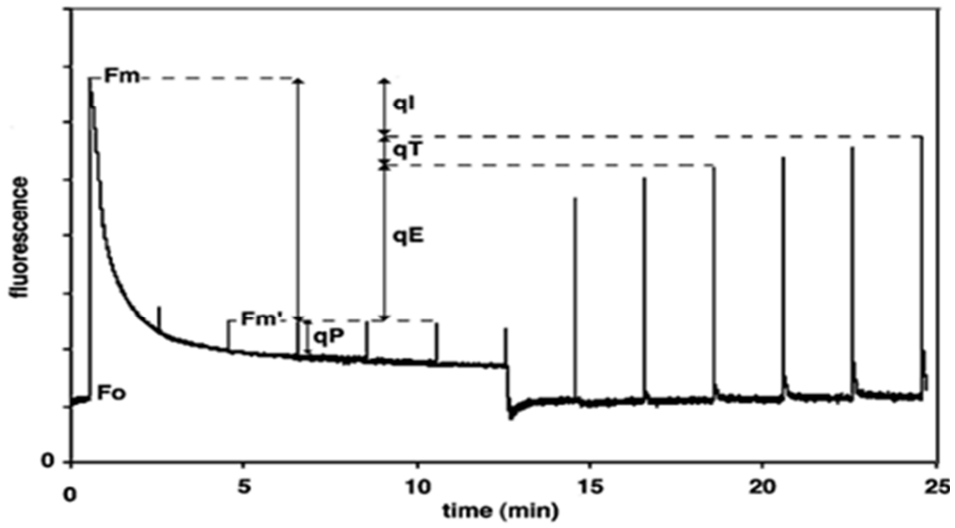

Figure 10: A typical chlorophyll fluorescence measurement, the values of qI, qT, qE, qP, F_0, F_M' and F_M are depicted (Niyogi et al., 2001)

NPQ can be kinetically divided into the three components: high-energy-state quenching (**qE**), the photoinhibitory quenching (**qI**) and fluorescence quenching caused by state transitions (**qT**). A typical procedure for measurements of these NPQ components by chlorophyll fluorescence is depicted in Figure 10. As one can see, if there is only weak measuring light, minimal fluorescence ($\mathbf{F_0}$) is observed. However, when the saturating pulse of light is induced, photosynthetic reaction centers become closed and a maximum level of fluorescence in dark is observed ($\mathbf{F_M}$). Subsequent continuous illumination with moderately excess light causes combining of the effects of photochemical quenching (**qP**) and NPQ which results in decrease in fluorescence yield. The value of NPQ can be calculated as a difference between F_M and maximal fluorescence measured during illumination ($\mathbf{F_M'}$). NPQ is a sum of its components **qE**, **qI** and **qT** that can be resolved from kinetics of NPQ recovery in dark. (Niyogi et al., 2001)

3.2 Energetic qE quenching

The qE quenching is the major, rapid and usually pH – or light energy dependent component of NPQ. It is triggered at excessive light by a decrease in pH in thylakoid lumen. Recent research shows that ΔpH in lumen induces qE through protonation of light harvesting antennae proteins and de-epoxidation of xanthophylls in xanthophylls cycle. These two processes are able to cause a conformational change in the light-harvesting antennae of PSII – in other words, they switch the antennae into a quenched state with a low fluorescence yield (Gilmore, 1997).

There are two main types of xanthophyll cycle in photothrops. The first type, violaxanthin cycle, typically present in plants, green algae and brown algae, catalyze of

violaxanthin into zeaxanthin via antheraxanthin. The second xanthophyll cycle is diadinoxanthin cycle catalyzing the conversion of diadinoxanthin to diatoxanthin - it can be found in diatoms and other algae. Interestingly, it was observed that some eukaryotic algae are able to use both cycles under certain conditions (Lohr, 1999). Additionally, another xanthophyll, lutein, is also able to increase the efficiency of qE (Pogson, 2000). Furthermore, third type of xanthophyll cycle, which involves lutein-5,6-epoxidase has been observed in a parasitic plant - c*uscuta* species (Bungard et al., 1999). There is a variety of proteins that are necessary to control qE. For example PsbS protein that is a member of the LHC protein super family is essential for qE in plants (Li et al., 2000).

As it was already stated, there are different mechanisms of NPQ throughout the photosynthetic organisms. I would like to introduce the basic models of this form of photoprotection throughout the higher plants, mosses, green algae and diatoms.

3.3 NPQ mechanism in higher plants

A model for NPQ in higher plants has been first introduced in 1992 (Ruban et al., 1992) and although it has been changed since that time a lot, its basics are still valid. NPQ in higher plants relies on trigger (ΔpH), xanthophyll cycle, PsbS protein and the state of LHC aggregation. The induction of NPQ in higher plants is dependent on the violaxanthin cycle that catalyzes reversible de-epoxidation of violaxanthin through antheraxanthin to zeaxanthin (Yamamoto et al., 1962). The forward reaction takes place under high light and it is catalyzed by the enzyme violaxanthin de-epoxidase (VDE). The drop of pH in lumen during the period of intensive irradiation causes VDE activation and the enzyme is able to bind to the thylakoid membrane. The backward reaction occurs under low light or in darkness and it is catalyzed by zeaxanthin epoxidase (ZE) usually working at neutral or slightly basic pH-values. The synthesis of zeaxanthin from violaxanthin in leaves takes minutes, but the backward

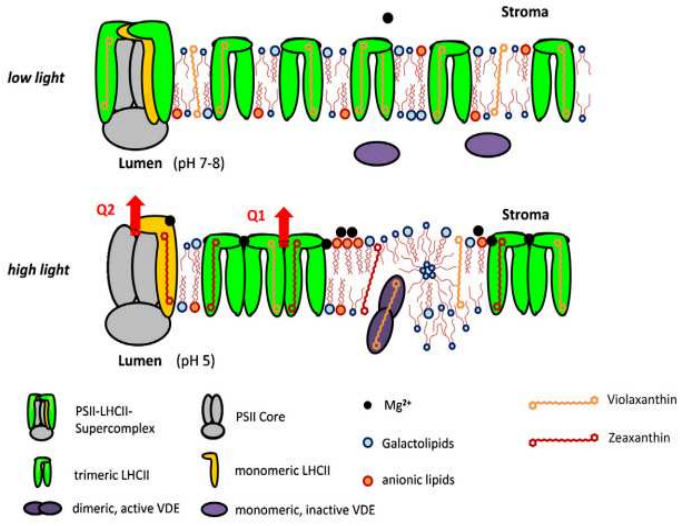

Figure 11: A schematic overview of the NPQ process in higher plants (Goss and Lepetit, 2014)

reaction takes hours. Therefore, zeaxanthin accumulated at high light is present in the dark for a longer period (Ruban, 2013). Zeaxanthin importance for NPQ mechanism was revealed already in 1990 (Demmig-Adams, 1990). The current model of NPQ in higher plants is summarized in Figure 11. Terms Q1 and Q2 correspond to the two quenching sites varying in the amount of zeaxanthin bound, red arrows signalize the dissipation of heat.

Apart from the zeaxanthin, there is another crucial component of NPQ in higher plants – PsbS protein. The structure of this protein contains four very hydrophobic transmembrane helixes and it does not bind pigments. It has a dramatic effect on NPQ - mutants lacking PsbS protein showed no rapidly forming NPQ (Li et al., 2000). It has been proposed that PsbS functions as a ΔpH transducer on the antennae.

3.4 NPQ mechanism in mosses

Mosses can be understood as an evolutionary link between land plants and aquatic species. *Physcomitrella patens*, a model organism of mosses, contains PsbS – protein necessary for NPQ in higher plants, together with LhcSR protein, which have similar function as PsbS in higher plants. It could be implied that land plants evolved a mechanism dependent only on the presence of PsbS before they lost LhcSR protein (Alboresi et al., 2010). Moreover it was proven that mutants lacking one of these proteins have reduced NPQ values, consequently these two proteins must somehow cooperate during the mechanism of NPQ in mosses. The mechanism of NPQ in *P. patens* is also highly dependent on the presence of zeaxanthin (Pinnola et al., 2013). Other measurements proved that NPQ mechanism results in reduced probability of triplet chlorophyll state formation (Carbonera et al., 2012).

3.5 NPQ mechanism in green algae

The basic mechanism of NPQ in green algae is similar to higher plants. It includes violaxanthin cycle, formation of the proton gradient and LHCII aggregation. In contrast to vascular plants, there is a higher importance of state transitions in green algae, and their primary function is to balance the excitation energy between PSII and PSI. Moreover state transitions play a crucial role in the regulation of linear and cyclic electron flow throughout chloroplasts (Allen, 1995).

There are other important differences in the mechanism of NPQ between green algae and vascular plants. For example most of the thylakoid membranes of green algae are not differentiated into grana and stroma region. (Gunning, 1999) and also some PSII antenna

proteins are missing. The biggest difference is lack of PsbS protein in most green algae; its function is substituted by the proteins from LhcSR family. Additionally, the model organism of green algae, *Chlamydomonas reinhardtii* showed NPQ only in high light acclimated cells, in contrast to constitutively induced NPQ in higher plants. There are also differences in NPQ between the green algae themselves. For instance, species of *Chlorella saccharophila*, *Chlorella vulgaris* and *Bracteacoccus minor* have the mechanism of NPQ dependent on zeaxanthin, whereas in species of *Tetracystis aeria*, *Pedinomonas minor* and *Chlamydomonas Reinhardtii* no violaxanthin de-epoxidation is exhibited or it is unrelated to the formation of NPQ. It could be concluded that NPQ in green algae is related or unrelated to the xanthophyll cycle, even though the species have comparable pigment composition (Goss et al., 2015).

3.6 NPQ mechanism in diatoms

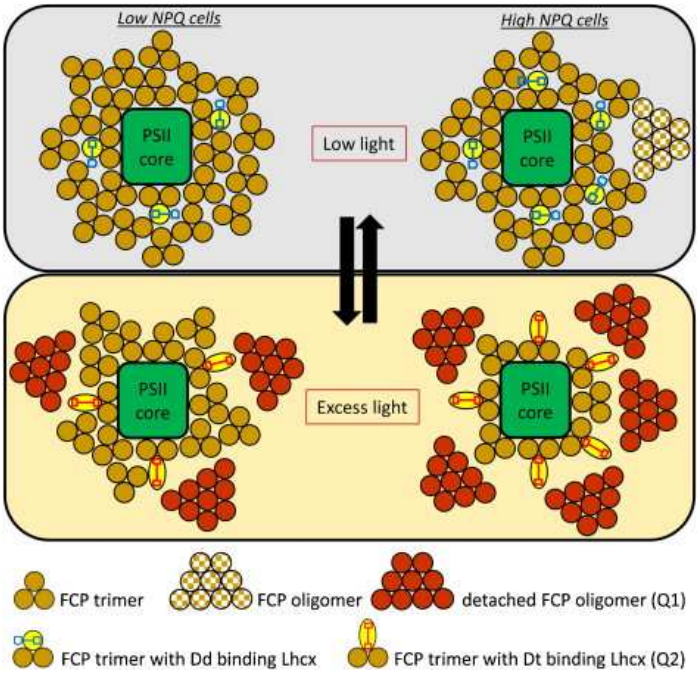

Figure 12: Model of NPQ in diatoms depicting several structural rearrangements in the PSII antennae after transfer from low light intensities to excessive light (Goss and Lepetit, 2014)

Diatoms chloroplasts are of secondary endosymbiosis origin from a red algal ancestor (Keeling, 2013). The mechanism of NPQ in diatoms differs from above mentioned mechanisms. It is hard to differentiate the qE and qI components of NPQ in diatoms due to extremely rapid relaxation of NPQ in comparison to higher plants. The proton gradient is involved in NPQ formation, but in contrast to green algae and higher plants, ΔpH is unable to trigger NPQ without presence of xanthophyll cycle (Lavaud et al., 2002). Photoprotective xanthophyll cycle is represented by conversion of diadinoxanthin to diatoxanthin (Dd-Dt cycle) by an enzyme diadinoxanthin de-epoxidase. The NPQ process depends on the antenna complexes – fucoxanthin-chlorophyll *a/c* proteins (FCPs). Moreover the measurements performed with *Cyclotella meneghiniana* shows two

NPQ components: qE(1) relaxing rapidly in the dark and qE(2) which is present in darkness and it is connected to the presence of Dt (van Amerongen et al., 2014). *Phaeodactylum tricornutum* is capable of forming NPQ three to five times larger in comparison with vascular plants (Ruban et al., 2004). The mechanism of NPQ in diatoms is depicted in Figure 12.

3.7 NPQ mechanism in other algae

Chrysophytes exhibit functional NPQ dependent on violaxanthin cycle (Dimier et al., 2009) and additionally in some of these algae also Dd was found, but no conversion from Dd to Dt was detected (Tanabe et al., 2011). The NPQ mechanism relying on violaxanthin cycle was also found in recently discovered alga *C. velia* (Kotabova et al., 2011). Dinophytes shows Dd-Dt cycle involved in NPQ (Brown et al., 1999). In contrast to all above mentioned algae, Cryptophytes exhibit completely different NPQ mechanism. While lacking a xanthophyll cycle, they show a rapidly inducible and reversible proton gradient – dependent NPQ located in LHC antennae. Consequently, Cryptophyte species *R. salina* exhibit fast induction and relaxation kinetics similarly to the proton gradient-dependent qE component of NPQ in higher plants. (Kana et al., 2012)

4 Chromera velia

4.1 Life cycle

C. velia is a unicellular photosynthetic organism which belongs to the superphylum Alveolata. This alga has been isolated from stony coral (*Plesiastrea versipora*) near the eastern coast of Australia (Moore et al., 2008). *C. velia* is a close relative od apicomplexan parasites, organisms which have unpigmented chloroplast called apicoplast. From this reason it constitutes an important evolutionary link between photosynthetic algae and heterotrophic parasites (e.g. *Plasmodium falciparum*). The life cycle of *C. velia* involves three life stages. The coccoid form (spherical, immotile but multiplying cells) is predominant when the culture is found in the stationary phase. If the culture is growing exponentially, the second form – flagellate occurs. When there is unfavorable environment an organism is found in the cystic form (Obornik et al., 2011). The chloroplast of this species is bound by four membranes and each cell usually contains one or two of them with the thylakoids in the stack of three or more. The major pigments in *C. velia* are chlorophyll *a*, violaxanthin and isofucoxanthin-like carotenoid. Additionally under certain conditions also zeaxanthin was detetected (Kotabova et al., 2011). *C. velia* can be endosymbiotic in coral larvae (Cumbo et al., 2013), but it can also become parasitic in the flagellate state when the organelles needed for invasion into the host are formed (Obornik et al., 2011).

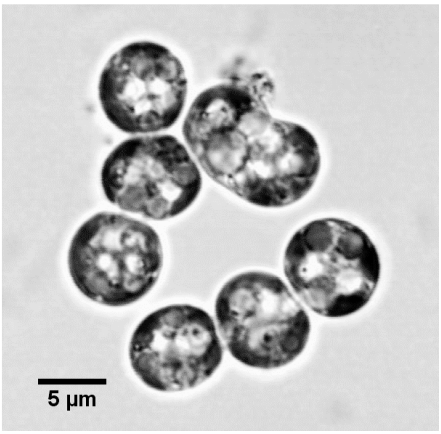

Figure 13: Cells of C. velia – magnification 100 x (Photo by Ing. Jaroslav Krafl)

4.2 Evolution

Chloroplasts of *C. velia* are supposed to origin from secondary endosymbiotic event from the free-living photosynthetic alga (Cavalier-Smith, 1999), they are related to the red algal chloroplast (Janouskovec et al., 2010). However, it is important to note that *Chromera* light harvesting complexes (CLH) complexes are encoded in nucleus from where antennae peptides migrate to function in the chloroplast. Therefore they can have a different evolution origin compared to proteins encoded in chloroplast.

A research with EST sequences has shown that *C. velia* contains peptide sequences closely related to diatoms, brown algae and dinoflagellates. Twenty three LHC homologs obtained from *C. velia* were aligned with other algal species. Seventeen LHCs were closest to FCPs of diatoms, brown algae and dinoflagellates, one sequence of LI1818/LI1818-like proteins (function as environment stress-induced protein complexes (Zhang et al., 2004) was related to green algae and chromalveolates, but only three LHC homologues grouped with LHCs of red algae (Pan et al., 2012).

In other study focused on light harvesting complexes, two different antenna complexes were observed and named Chromera Light Harvesting (CLH) complexes (Tichy et al., 2013). The first one was related to FCP antenna of diatoms and xanthophytes, and the second one (PSI with bound LHC) was similar to the one found in red algae (Tichy et al., 2013).

4.3 NPQ

Although *C. velia* lacks any other chlorophylls except chlorophyll *a* and uses only primitive type of RuBISCO, its photosynthesis represents highly efficient system (Quigg et al., 2012) that shows some similarities to higher plant photosynthesis (e.g. the presence of violaxanthin cycle (Kotabova et al., 2011)). *C. velia* cells are able to acclimate to a wide range of light intensities and tend to perform photosynthesis in maximal rates under various conditions. It has been suggested that *C. velia* can stimulate photorespiration (Quigg et al., 2012) and NPQ (Kotabova et al., 2011) in order to avoid photoinhibition. It is supposed that high CO_2 assimilation rates (under sinusoidal light regime) are enabled by activation of the oxygen consuming mechanism, which helps to maintain stable efficiency of RuBISCO. (Quigg et al., 2012). The cells grown under high light (300 photons $m^{-2}s^{-1}$) exhibit a slight increase of isofucoxanthin accompanied with a strong increase in violaxanthin when compared to the culture grown under medium light (120 µmol photons $m^{-2}s^{-1}$) regime (Mann et al., 2014). Moreover NPQ in *C. velia* is connected with very fast violaxanthin de-epoxidation to zeaxanthin (Kotabova et al., 2011). Zeaxanthin can be detected already one minute after light exposure and it is almost impossible to observe the intermediate of the de-epoxidation, antheraxanthin. The transformation is driven by proton gradient in the thylakoid membrane and is unusually fast in comparison to vascular plants. The forward reaction is reversible in the dark, when zeaxanthin is partly converted back to violaxanthin during 20 minutes of relaxation.

When NPQ of *C. velia* was compared with NPQ of *Nannochloropsis limnetica*, *C. velia* exhibited very high dissipation of energy, whereas *N. limnetica* had limited NPQ capacity and subsequently the excessive irradiation caused photoinhibition of PS II in this species (Kotabova et al., 2011). Zeaxanthin formation and NPQ in *C. velia* exhibit similar features: comparable kinetics and pH dependency. In fact, there is linear correlation between NPQ and zeaxanthin formation, therefore an inhibition of the VDE lead to equal reduction in NPQ (Kotabova et al., 2011).

5 Materials and Methods

5.1 Cell growth

Chromera velia (strain RM12), was grown in artificial sea water medium with addition of f/2 nutrients (Guillard and Ryther, 1962). Cells were cultivated in glass tubes at 28°C, in the continuous light regime of 100 µmol m^{-2} s^{-1} and bubbled with air. The cell density was measured from three biological samples every second day. The cells were sonicated for 45 s using ultrasonic bath prior to analysis on Beckman coulter (Multisize 4, USA) equipped with 50 µm aperture. Specific growth rates (µ, h^{-1}) were calculated from $\mu = (\ln c - \ln c_0)/ t\text{-}t_0$, where *c* is the final amount of cells in the exponential phase and c_0 is the start amount of cells in the exponential phase; *t* is the end time of exponential phase and *t0* is the start time of the exponential phase.

5.2 Membrane solubilization

Culture of *C. velia (OD at 750 nm 0.5-0.8)* was centrifuged (4 °C/ 7000 rpm/ 10 min) and the resulting pellet was resuspended in the medium, put into the 2 ml vials and again centrifuged (4 °C/ 5000 rpm/ 5min, Eppendorf centrifuge 5804 R, USA). The following procedure was performed in the dark and on ice. The pellet was resuspended in 400 ml 25mM HEPES – pH 7.8. Ballotini beads (0.1 – 0.2 mm, Biospec, USA) and zircon beads (0.1 mm, Biospec, USA) were added in the ratio of 1:1 and the cells were broken using bead beater (Mini Bead Beater, BioSpec, USA) 15 shaking cycles, in the intervals of 10 s with 2-min breaks for cooling the suspension on ice. The beads were washed with HEPES and membranes were separated from the cell extract by centrifugation (4°C/ 18000 rpm/ 20 min, Sigma3K30, Germany). Supernatant was discarded and the pellet of thylakoid membranes was resuspended in HEPES. Membranes were centrifuged under the same conditions, supernatant discarded and then thylakoid membranes were solubilized with β – DDM (1-2 %) in HEPES and incubated for 1 hour on ice. Afterwards the solubilized membranes were centrifuged (4°C/ 13000 rpm/ 10 min) and supernatant was ready to use in isolation techniques.

5.3 Sucrose density centrifugation

The fresh continuous 5%-15%/(20%) sucrose density gradient was prepared in β – DDM/HEPES buffer (25mM HEPES, pH 7.8, 0.04% β – DDM) using a locally made

gradient mixer system or by pouring the solution of 5% sucrose on top of the solution of 15% sucrose and putting the tubes into the horizontal positions for 3 hours at 5°C. The final supernatant from section 5.2 was loaded on top of the gradient. The ultracentrifugation was performed with rotor SW 28 (for 40ml tubes) and rotor SW 40 Ti (for 12ml tubes) by L8-M ultracentrifuge (Beckmann, USA) at 4°C/ 20 h at the speed of 141118 g and 284061 g, respectively. Resulting bands after centrifugation were pipetted into the separated vials.

5.4 IEF

Separation of membrane proteins by isoelectric focusing (IEF) was done by Multiphor II system (GE Healthcare Life Sciences, USA). Eight electrode strips were cut to fit into the inner width of the apparatus tray. These strips were soaked in 10 ml of 2% ampholine solution and placed three on top of each other at both ends of the tray. Afterwards the gel-ampholyte slurry was prepared from H_2O (97.5 mL), ampholytes (2.5 ml), glycine (1 g), β-DDM (600 ul of 10% solution) and Sephadex 75 (4.6 g). The tray was placed on the balance scales and the ampholyte slurry was poured into the tray and air bubbles were gently removed. Excess water (37 g) was evaporated from the tray during three hours by fan. 30 ml of 0.1% Triton X-100 solution was applied in a thin layer onto the gel and the tray was placed on the cooling plate (9°C). One electrode strip was soaked in anode solution of 5.3% H_3PO_4 and another electrode strip was soaked in cathode solution of 1M NaOH. Both of them were correspondingly applied on the strips in the tray. After applying the electrode holder with electrodes to the tray, the pre-focusing (45 min – 2 hours) was done with the current of 13 mA and voltage of 600V to stabilize the apparatus at 8 W.

The sample was prepared according to section 5.2. The sample applicator was placed approximately two cm from the cathode and all the gel from it was removed and mixed with the sample. Subsequently, the gel was put back into the applicator area and IEF (pH range of 2.5 – 5) was run for 17 hours. The bands were collected using a thin spatula and elution buffer (25mM HEPES and 0.1 % β-DDM) was used to elute the protein complexes.

5.5 FPLC – Ion Exchange Chromatography

Thylakoid membranes of *C. velia* were solubilized according to section 5.2 from 600 ml of *C. velia* culture with 1.5 % β-DDM used for solubilization. The solubilized material was loaded into the 2ml sample loop of FPLC system (Pharmacia, Biotech, Sweden). Protein separation by IEC was performed on continuous bed anionic exchange column UnoQ-6 (volume 6 ml, BIO-RAD, Italy) and FPLC system controlled by programmer GP – 250 Plus

(Biotech, Sweden) equipped with the FPLC flow through UV/Vis detector (Shimadzu – SPD –20AV prominence, USA), where absorbance was recorded with at two wavelengths – 450 and 670 nm. The following method was applied: at first, column was equilibrated with buffer A (20 mM HEPES, 0.04 % β-DDM, pH 8), afterwards sample was eluted with a linear gradient of $MgCl_2$ formed by mixing of buffer A with buffer B (20 mM HEPES, 0.04 % β-DDM, 0.5 M $MgCl_2$, pH 8) during 45 min, 50% of buffer B was applied on the end of this phase. Then, 100% buffer B was used for 20 minutes to ensure compete elution of proteins. The whole procedure was done at 4°C with the flowrate of 0.8 ml min^{-1}.

5.6 Absorption spectra

Absorption spectra of the isolated pigment-protein complexes were analyzed by Unicam UV /VIS 500 spectrometer (Thermo spectronic, UK) in quartz cuvettes (Type 18/B, Path length 10, match code 6, Chromspec, CZ) with a bandwidth of 1.0 nm and scanning speed of 120 nm min^{-1}.

5.7 Low temperature fluorescence spectra

Low temperature fluorescence spectra of isolated fractions from sucrose density gradients (section 5.3) were measured in a reflection mode by diode array spectrofluorometer SM-9000 (PSI, Czech rep.). The isolated complexes were fixed in the sample holder and immersed into the dewar vessel filled with liquid nitrogen (T = 77 K). The fluorescence spectra were measured using 425 nm and 457 nm excitation light (spectral bandwidth 20 nm) with absolute emission accuracy of 0.8 nm.

Low temperature fluorescence spectra of IEF fractions (section 5.4) were measured using a Jobin Yvon FluoroMax-3 spectrophotometer (Horiba, USA) equipped with nitrogen bath bath cryostat. The diluted sample (OD<<0.1) was carefully injected between two glass windows (separated by a spacer and kept in place by a metal spring) that was then quickly immersed in the liquid nitrogen bath. After few minutes (time necessary for the sample to reach 77 K) the nitrogen bath was aligned to the spectrofluorometer. Spectra were measured for excitation at 435 nm (5 nm spectral bandwidth) and detected with spectral resolution of 1 nm. The spectra were corrected for different intensity automatically.

Low temperature fluorescence spectra of IEC fractions (see section 5.5) were measured by Aminco Bowman series 2 spectrofluorometer (Thermo Fisher Scientific, USA) with the excitation of 440 and 455 nm (4 nm bandwidth) and recorded with spectral bandwidth of 1 nm between 650 nm and 800 nm.

5.8 SDS-PAGE

The protein composition of the isolated complexes was determined by SDS-PAGE using 12% polyacrylamide SDS gel in the BIO-RAD apparatus (Mini – Proteam Cell, Italy). The gels were stained either by Coomassie Brilliant Blue or by silver stain (ProteoSilver Silver Stain Kit, Sigma-Aldrich, USA). The molecular weights were estimated according to the applied ColorPlus Prestained Protein Marker, Broad Range (7-175 kDa) (New England Biolabs).

5.9 Pigment analysis by HPLC

Isolated pigment protein complexes were extracted using 100% methanol and separated on Phenomenex column (Luna 3µ C8, size 100 x 4.60 mm) at gradient of 0.028M ammonium acetate/MeOH (20/80) (flow rate of 0.8 ml/min, t = 35°C see (Jeffrey and Vesk, 1997)). Pigments were quantified based on their absorption at 440 nm and their extinction coefficients.

5.10 Nonphotochemical fluorescence quenching in native cells

In vivo quenching was measured by chlorophyll *a* fluorometer FL 3000 (PSI, Brno, Czech rep) with a pre-setup measuring protocol. Orange light (intensity of 600 µE, wavelength of 625 nm) was applied to induce nonphotochemical quenching of fluorescence in the whole cells of *Chromera velia*, which were previously dark adapted for 20 min. The effect of uncoupler on the fluorescence quenching was examined by adding NH_4Cl (final concentration of 0.7 mM) during a different period of the measuring protocol (start - dark, 10%, 20%, 30%, 40% of the protocol duration). *C. velia* cells with optical density of 0.615 (for λ = 750 nm).

5.11 Nonphotochemical fluorescence quenching in isolated antennae

The extent of nonphotochemical fluorescence quenching in the isolated CLH complex from sucrose gradient was measured using chlorophyll *a* fluorometer FL 100 (PSI Czech rep., blue excitation at 464 nm, intensity 184 µE). Fluorescence quenching was induced by dilution of 24 µl sample (CLH antennae fraction F2 in 25 mM HEPES, pH 78, 0.04 % *n*-Dodecyl β-D-maltoside) in the 948 µl buffer (10mM HEPES, 10 mM sodium citrate, pH 7.6) during continuous stirring. Final concentration of β-DDM was 15 µM. The pH of the solution was reduced to pH 5.5 (Figure 23) by 5% HCl (4.9 µl) addition to trigger pH –

induced quenching. In the pH – dependency NPQ experiment (Figure 24) the pH of the solution was gradually (in the 25 %, 40 % and 55% of the protocol) reduced to pH 6.5, 6 and 5.5 by adding 5% HCl in the amount of 2.2 µl, 1.3 µl and 1.4 µl, respectively. The reversibility of quenching was tested by β-DDM addition (final concentration of 200 µM) at the end of the protocol.

6 Results

6.1 *C. velia* growth curve

Before protein isolation, optimal growth of *C. velia* cells was tested. We have found out that *C. velia* cells grew exponentially till approximately 12 million cells per ml; afterwards they went into the stationary phase (see Figure 14). The sudden change into the stationary phase (day 6) was caused by high pH of culture (pH of 9.5). The experiment was repeated three times, the third repetition (C.V.3) exhibited smaller number of cells due to presence of stacked cells which were impossible to separate even after the sonication.

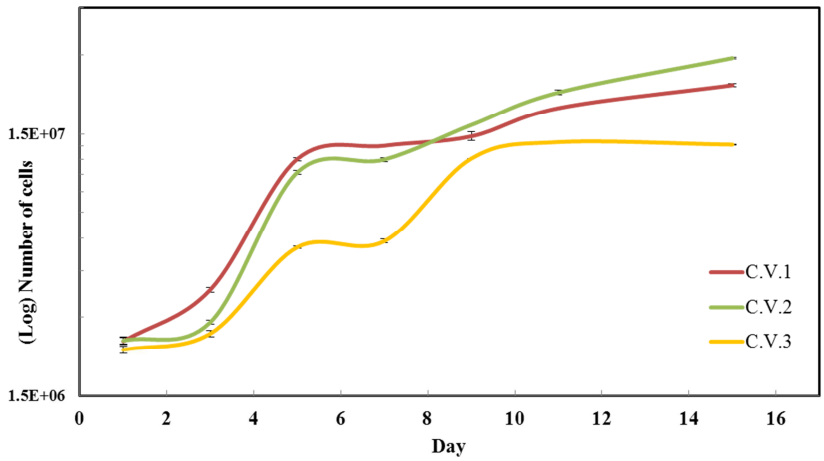

Figure 14: C. velia growth curves from three biological samples (C.V.1-C.V.3), number of cells measured using Beckman coulter (Multisizer 4, USA)

Specific growth rates (μ, h^{-1}) were calculated from $\mu = (\ln c - \ln c_0)/ t\text{-}t_0$. The doubling time ($t_d = \mathrm{Ln}\ 2)/\mu$) of *C. velia* growth was determined to be 32 hours (see Tab. I). Cells for isolation and measurements were always harvested either on day 4 or on day 5 to ensure the exponential phase. For further measurements the culture was always harvested either 4^{th} or 5^{th} day after dilution.

Tab I: Specific growth rates of *C. velia* under the continuous light regime of 100 µmol m^{-2} s^{-1}

	C.V.1	**C.V.2**	**C.V.3**
µ [hours^{-1}]	0.02	0.02	0.01
t_{double} [hours]	32.04	28.00	48.78
µ [days^{-1}]	0.52	0.59	0.34
t_{double} [days]	1.33	1.17	2.03

6.2 Protein isolation by sucrose density gradient centrifugation

Thylakoid membrane antennae proteins were separated on linear sucrose density gradient (see section 5.3). Two methods have been tested for isolation and we observed

separation of antennae proteins into two distinct upper bands (see representative results in Figure 15) in both of them. In the first isolation (2% β-DDM used for solubilization – see section 5.2, linear 5-20 % sucrose gradient in 25 mM HEPES, 0.04 % β-DDM, 40ml- tube, SW 28, 141118 g, 20 h) we obtained 3 main fractions. Upper fraction F1 contains many free pigments (section 6.2.2), fraction F2 corresponds to **C**hromera **L**ight **H**arvesting complexes (CLHc) and fraction in the lower part of the gradient (not named in Figure 15) corresponds to bigger complexes possibly containing photosystem I. Only the upper two bands (F1 and F2) were used for further measurements. F2 was used for measurement of nonphotochemical quenching in isolated complexes (refer to section 6.5).

We have optimized the method in the following conditions –the amount of β-DDM required to solubilize the antennae proteins was refined after experiments with dilution series and it was lowered to 1 - 1.5 %; smaller ultracentrifugation tubes (12ml) were used for better distinction of the bands and increased g-force of 284061 g lead to better resolution. The setup resulted in the improved pigment-protein separation as you can see in Figure 15 panel B. These data represents sucrose density gradient of *C. velia*, which was subsequently used for further identification of pigment-protein complexes by means of SDS-PAGE (refer to section 6.2.4). The gradient showed again separation into two upper bands, but the third one was almost not visible, which is caused by insufficient amount of detergent for solubilization of photosystems.

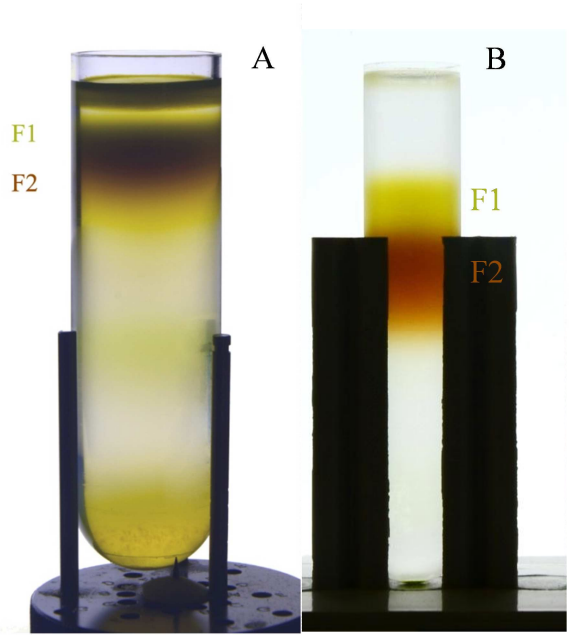

Figure 15: Isolation of thylakoid membrane pigment-protein complexes on linear sucrose density gradient. Panel A: Isolation of proteins on sucrose gradient ranging from 5 to 20% in 40 nm tube, solubilization was done with 2% β-DDM; Panel B: Isolation of proteins on linear sucrose gradient ranging from 5 to 15% in 12 ml tube, solubilization was done with 1.5% β-DDM

6.2.1 Absorbance spectra of antennae fractions

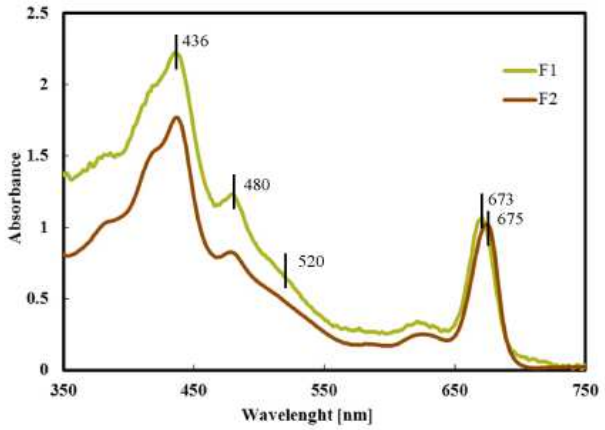

Figure 16: The absorbance spectra of fractions 1 and 2 isolated from sucrose density gradient (see Figure 15A). Spectra were measured by Unicam UV /VIS 500 spectrometer (Thermo spectronic, UK)

The isolated antennae fractions from sucrose gradients (Figure 15) were further characterized. The absorbance spectra (Figure 16) showed differences in composition of studied complexes. In both fractions, the maximum peak of 436 nm together with maximum of 673 nm (675 nm) corresponds to the absorption of chlorophyll *a*. The other two maxima of 480 nm and 520 nm correspond to carotenoids absorption, namely violaxanthin and isofucoxanthin, respectively. All spectra are normalized to the chlorophyll *a* maximum in the red part of the spectra and zeroed at 730 nm. Absorbance spectra have indicated that fraction F1 contains higher amount of both carotenoids.

6.2.2 Low temperature fluorescence spectra of antennae fractions

Low temperature fluorescence emission spectra of isolated antennae fractions from sucrose gradients (Figure 15A) have shown typical properties. Fraction F1 had maximum at 680 nm, F2 was red-shifted with maximum of 682 nm.

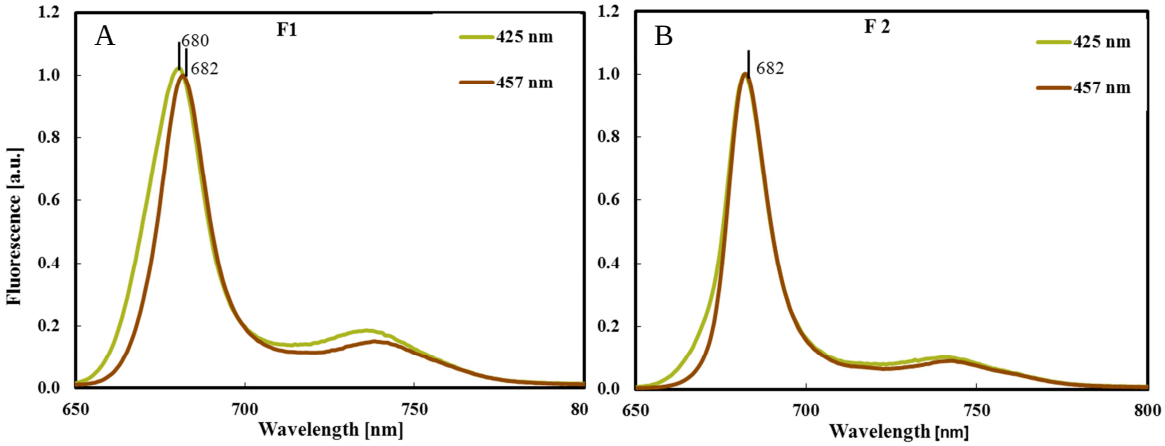

Figure 17: Fluorescence emission spectra of fractions F1 and F2 isolated from sucrose gradient at 77K, excitation with wavelengths of 425 nm and 457 nm measured by Optical spectrometer SM-9000 (PSI, Czech

rep.; Panel A: Fluorescence emission spectra of fraction F1; Panel B: Fluorescence emission spectra of fraction F2

6.2.3 Pigment composition of isolated antennae fractions

HPLC method was used to find the differences in pigment composition in isolated complexes from sucrose gradients (section 6.2). The following pigments were detected: chlorophyll *a* (retention time 25.1 min), violaxanthin (retention time 11.7 min) and isofucoxanthin (retention time 14.2 min). Numbers 1, 2 and 3 (Figure 18A) correspond to the violaxanthin, isofucoxanthin and chlorophyll *a*, respectively. Figure 18B shows the relative content of violaxanthin, isofucoxanthin and chlorophyll *a* to the total pigment content of antennae fractions F1 and F2. F1 contained relatively higher amount of violaxanthin in comparison to other pigments. In contrast, the amount of other carotenoid, isofucoxanthin was comparable in both fractions. F2 was enriched in chlorophyll *a* content. .

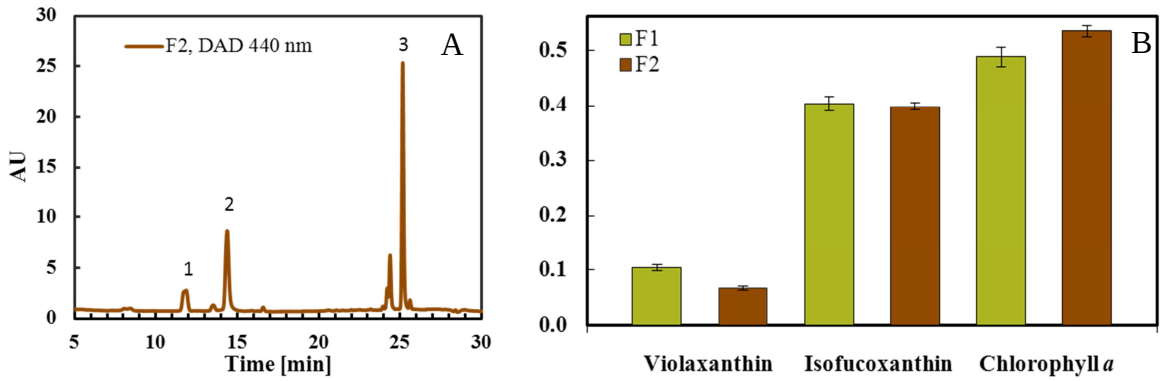

Figure 18: The results of HPLC analysis of isolated antennae fractions F1 and F2 from sucrose gradient, the analysis was performed on Phenomenex column (Luna 3µ C8, size 100x4.60 mm) – refer to section 5.9; Panel A: A representative chromatogram of fraction F2, number 1 corresponds to violaxanthin, number to corresponds to isofucoxanthin and number 3 corresponds to chlorophyll a.; Panel B: the relative content of violaxanthin, isofucoxanthin and chlorophyll a to the total pigment content;

6.2.4 Protein composition of antennae fractions

Isolated bands from sucrose gradient (Figure 15B) were characterized by SDS PAGE. Resulting zones on the gradient were furtherly divided – F1 into S1, S2 and F2 into S3, S4, S5, the lower fraction of the gradient was named S6 and the bottom S7 (see Figure 19, panel A). In order to characterize the pigment-protein complexes more precisely, border fractions S2 and S4 were discarded to avoid mixing of the bands and all the fractions were approximately ten times concentrated using Amicon filters (100 kDa). Fractions were loaded on the 12% polyacrylamide gel. The first zone (S1) contained several proteins with

molecular weight between 30 and 46 kDa. Further antennae protein zones (S3 and S5) showed two groups of antenna proteins. The molecular weight of larger antenna protein was around 20 kDa, smaller antenna protein was around 18 kDa. Fraction S6 did not reveal any protein pattern and fraction S7 was full of different proteins, which could correspond to some insolubilized material.

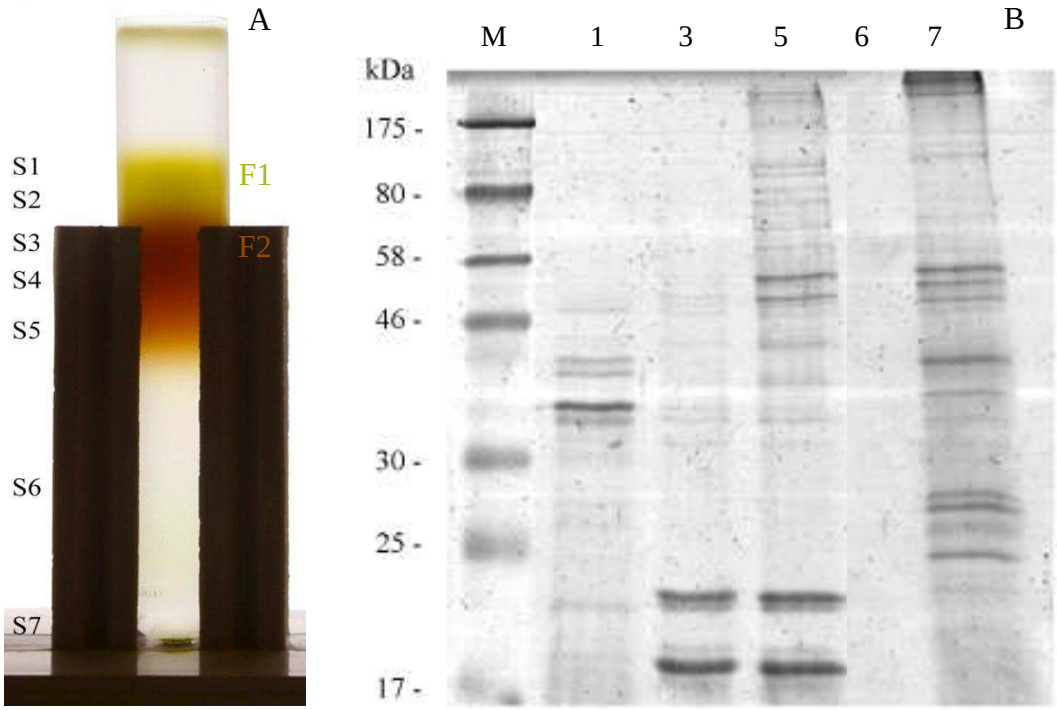

Figure 19: Protein composition of thylakoid membranes separated on linear sucrose density gradient (5-15% sucrose; Panel A: Sucrose density gradient (Figure 15B) with depicted fraction division to S1-S7; Panel B: Protein separation by SDS-PAGE (12% polyacrylamide gel), stained by Coomassie Brilliant Blue, M corresponds to protein ladder, numbers 1, 3, 5 and 7 represents fractions (S1, S3, S5 and S7) isolated on sucrose gradient.

6.3 Protein separation by isoelectric focusing

Proteins from solubilized thylakoid membranes (2% β-DDM, see section 5.2) of *C. velia* were separated by isoelectric focusing on the IEF gel. The resulting pattern on the gel from IEF is depicted in Figure 20A. The material was well solubilized and the gel shows two main groups of proteins (I and II). The first group (I) contained 4 fractions I1-I4 which correspond to the pI of 4 - 4.25 and the second group (II) contained 2 fractions I5 and I6 that exhibit pI around 5. The proteins with different pI were weakly visible within the groups as the concentration of the sample was too low for pronounced identification of the bands.

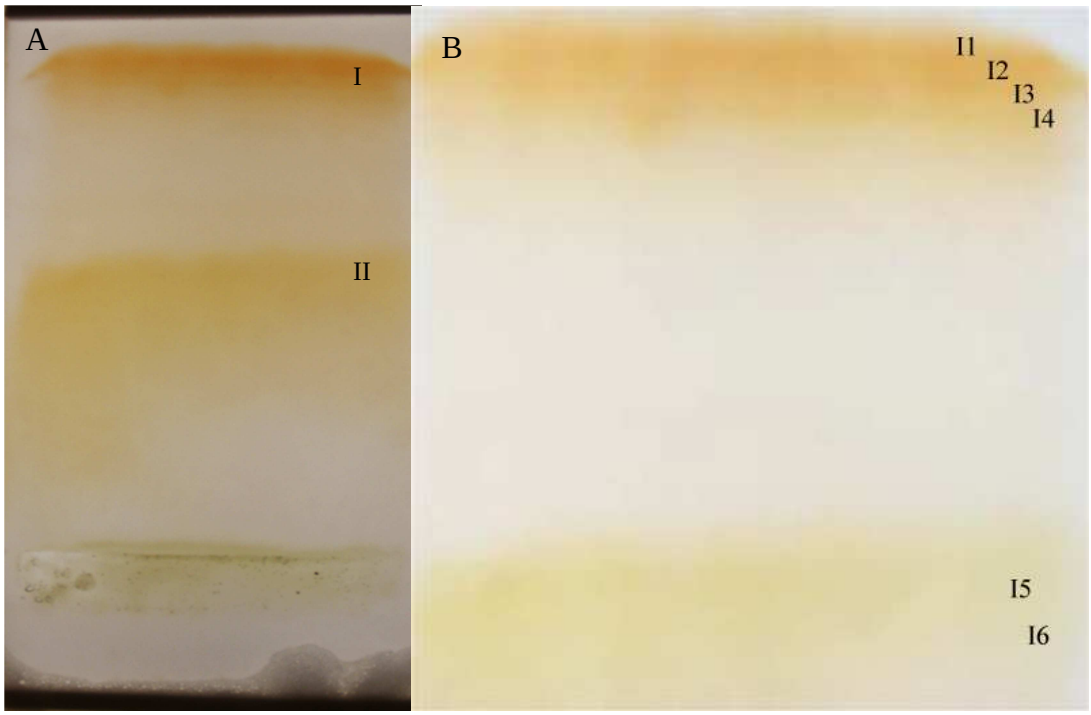

Figure 20: Separation of solubilized thylakoid membrane proteins (solubilization by 2% β-DDM) by isoelectric focusing, Panel A: Complete picture of IEF gel that has been done by Multiphor II system (GE Healthcare Life Sciences, USA; section 5.4), two main groups of proteins, I and II are marked; Panel B: Gel section characterizing bands : Magnification of the resulting protein bands, numbers 1-4 correspond to the first group of proteins with putative isoelectric points (pI) of 4-4.25, numbers 5 and 6 belongs to second group of proteins with pI around 5.

6.3.1 Low temperature fluorescence spectra of proteins isolated by IEF

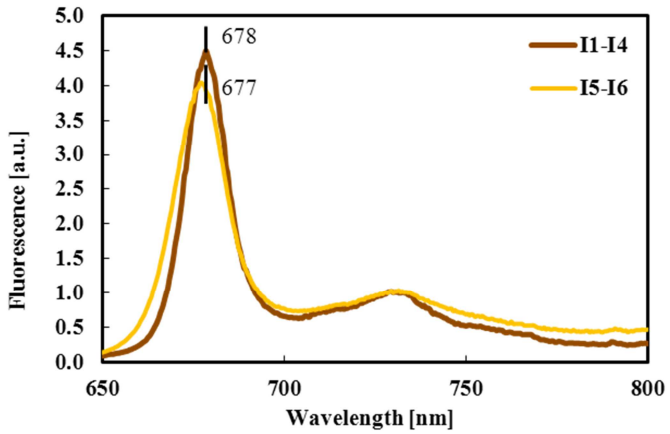

Figure 21: Low temperature fluorescence spektra of proteins isolated by IEF (Figure 16), fractions I1-I6 measured with excitation wavelength of 435 nm recorded by Jobin Yvon FluoroMax-3 spectrophotometer (Horiba, USA)

The low temperature fluorescence spectra were measured (see section 5.7) for proteins isolated by IEF (see Figure 20). The spectra showed the same profile for fractions I1-I4 and fractions I5-I6 as depicted in Figure 21, which supports the fact that these fractions have similar biophysical properties and they differ only slightly, maybe in amino acid composition. The

maxima were blue-shifted in comparison to fractions isolated on sucrose density gradient (see Figure 17), which usually indicates less intact samples.

6.3.2 SDS-PAGE of protein fractions isolated by IEF

Proteins isolated from IEF were ten times concentrated using Amicon filters (100 kDa) and then characterized by SDS-PAGE electrophoresis (on 12% acrylamide gel, for details see section 5.8). The resulting protein pattern of IEF fractions (Figure 22) revealed different proteins considering their molecular weight. Fraction I1 with the lowest pI, was very different from fractions I2-I4. These fractions contained a protein doublet at between 18-20 kDa resembling doublet hypothetical antennae proteins from Fig. 19. The other hypothetical antennae protein of 30kDa was missing in Fraction I2, and present in fraction I1 and I3. Hypothetical antennae protein doublet (18-20 kDa) in fractions I3 and I4 was enriched mostly by antenna proteins of 20 kDa, band I4 had also proteins of a lower molecular weight (~18kDa). Fractions I5 and I6 with higher pI at around 5 (see Fig. 20) seemed to be enriched in low molecular proteins (< 18 KDa).

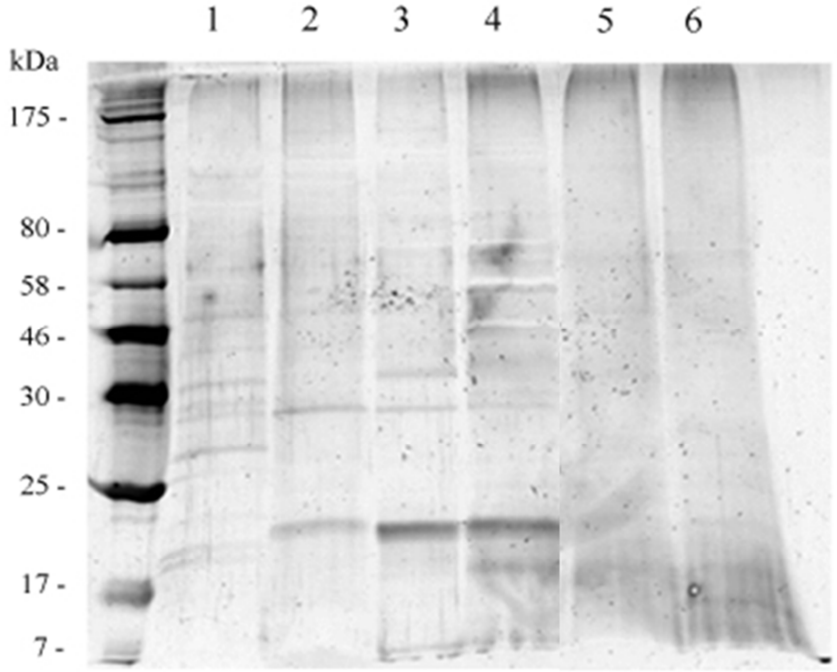

Figure 22: 12% polyacrylamide gel of C. velia proteins isolated by means of IEF, protein visualization was done by silver staining, numbers of wells 1-6 corresponds to the numbers of bands on IEF gel I1-I6 (see figure 20B)

6.3.3 Protein isolation by ion exchange chromatography

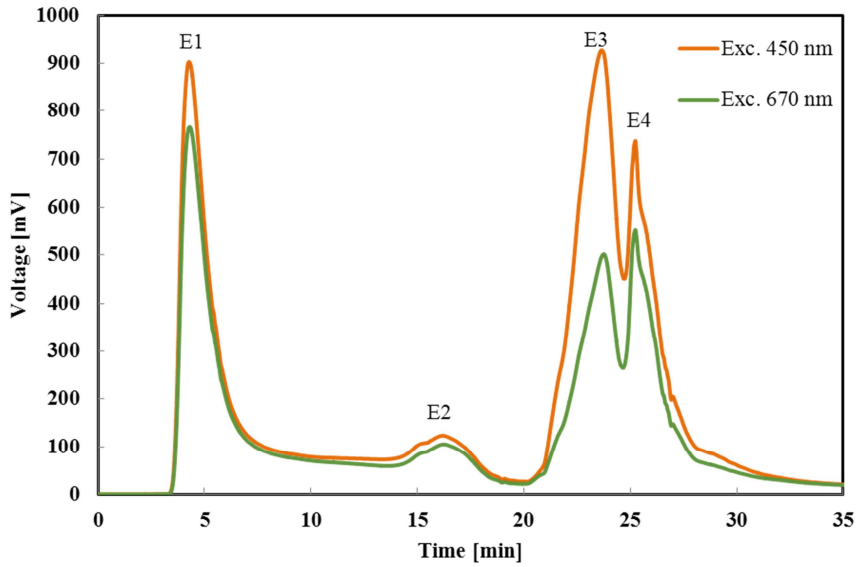

Figure 23: Elution profile of IEC method for C. velia thylakoid membranes (1% β-DDM used for solubilization. Absorbance was recorded at the wavelength of 450 nm and 670 nm – refer to section 5.5, proteins were separated into four fractions E1-E4

Solubilized thylakoid membrane proteins of *C. velia* were separated by FPLC with anionic-exchange chromatography column (see section 5.5). The column separated membrane proteins into four fractions E1-E4. The isolated fractions were subsequently characterized to resolve their protein and pigment composition (see section 6.4.1 and 6.4.2).

6.3.4 Absorbance spectra of fractions from IEC

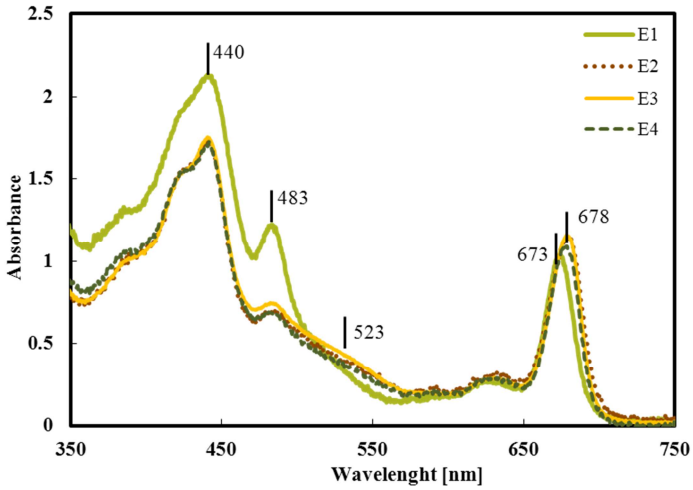

Figure 24: Absorbance spectra of fractions E1-E4 isolated by means of ion exchange chromatography (see Figure 19). Spectra were measured by Unicam UV /VIS 500 spectrometer (Thermo spectronic, UK) and normalized to 730 nm and chlorophyll a maximum.

Fractions from IEC (Figure 23) were characterized by absorbance spectra. Data indicated that fraction E1 had higher violaxanthin to chlorophyll ratio in comparison to other fractions as it was seen from 440 nm (chlorophyll *a*) and 483 nm (violaxanthin) absorption maxima. Other 3 fractions

(E2-E4) had similar absorbance spectra with relatively higher amount of isofucoxanthin absorbing at 523 nm in comparison to E1. The maximal emission in red region had shifted chlorophyll *a* maximum to 678 nm.

6.3.5 Low temperature fluorescence spectra of proteins isolated by IEC

Low temperature fluorescence spectra of fractions obtained from IEF (figure 23) showed that E1 is composed mostly from free pigments (usually peaking at 675 nm) but there are also some antennae proteins with maximum of fluorescence at 679 nm (see Figure 25). On the other hand, E2-4 had very similar fluorescence with the maximum of 685 nm which could suggest complexes of PSI and PSII. The following characterization by SDS-PAGE and CN-PAGE is required for better understanding of the pigment-protein complexes.

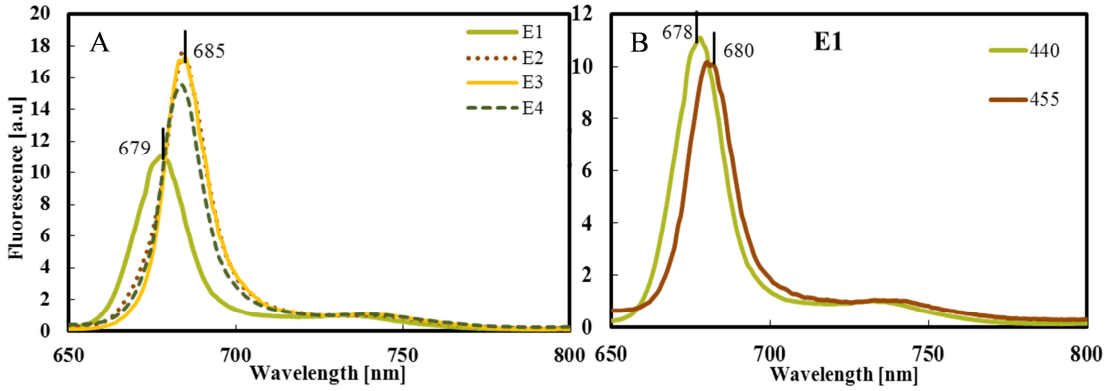

Figure 25: low temperature fluorescence spectra of fractions E1-E4 obtained from ion exchange chromatography, excitation wavelength 440 nm. Panel A: summary low temperature fluorescence spectra of fractions. Panel B: Low temperature fluorescence spectra of fraction E1 recorded at two excitation wavelengths (440 and 455 nm). Data were recorded using Aminco Bowman series (Thermo Fisher Scientific, USA) – see section 5.7; spectra were normalized to the wavelength of 730 nm

6.4 Nonphotochemical fluorescence quenching *in vivo*

Nonphotochemical quenching of fluorescence (NPQ) was induced by orange light (see Figure 26) in the whole cells of *Chromera velia* (see section 5.10). The value of NPQ was calculated according to the formula $(F_M'-F_M)/F_M'$ with the result of 0.723. The kinetics of the fluorescence decrease was fast, whereas observed fluorescence recovery in the dark was slow.

Role of pH in NPQ triggering was studied by adding a proton-gradient uncoupler (final concentration of 0.7 mM) to the whole cells of *C. velia* (see Figure 27) during a different period of the measurement (start - dark, 10%, 20%, 30%, and 40% of the protocol duration). The addition of uncoupler before light period lead to inhibition of NPQ and the fluorescence

value stayed constant. Addition of uncoupler during light phase of the measuring protocol lead to slow increase in fluorescence no matter at which time the uncoupler was added into the cells. The results correspond to the previous results with effect of pH (Kotabova et al., 2011).

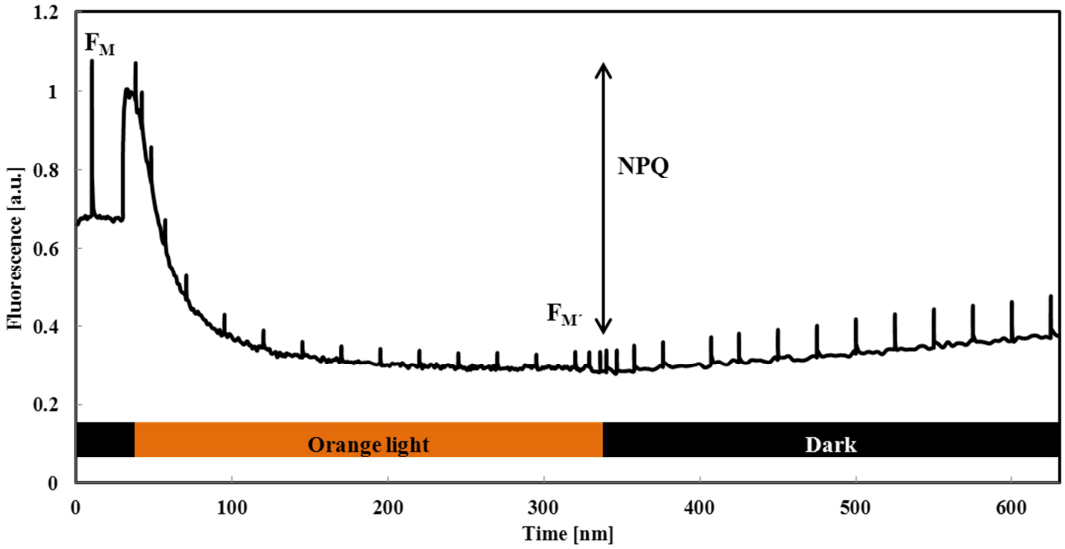

Figure 26: Fluorescence induction of C. Velia cells (dark adapted for 20 min) recorded on orange light. Data were measured by FL 3000 (PSI, Czech rep) F_M is a maximum level of fluorescence in dark caused by closed reaction centers after saturating light pulse; F_M' maximal fluorescence measured during illumination with orange light (600 µE), the bars depict the different phases of protocol, the dark phase at the end of the protocol leads to recovery of fluorescence quenching (for explanation of the protocol, refer to section 3.1 and 5.10, Figure 10.

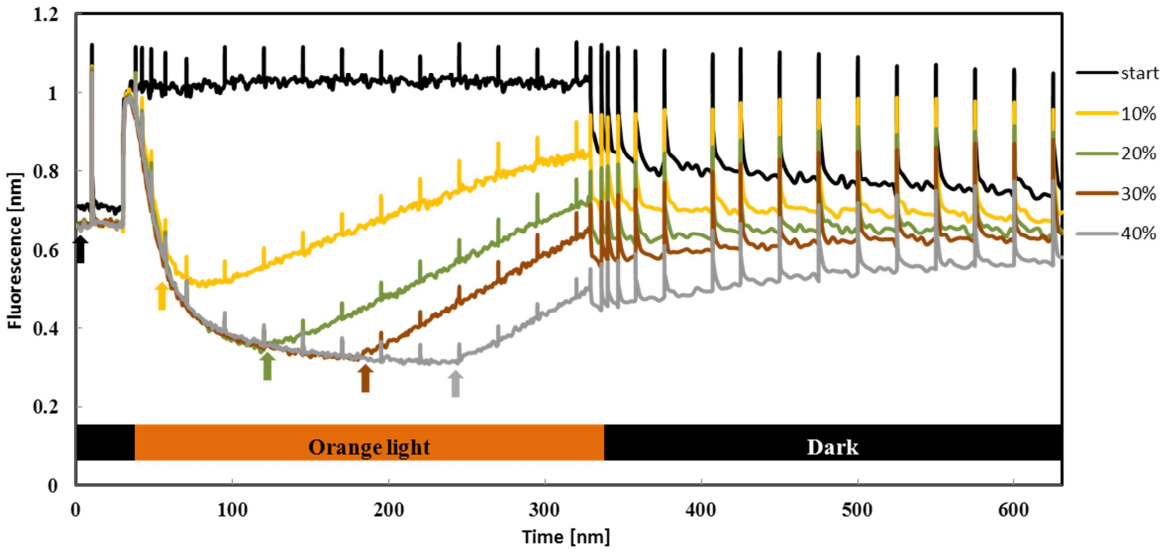

Figure 27: Changes in fluorescence induction after adding NH_4Cl into the sample with whole cells of C. velia (dark adapted for 20 min). Data were recorded by FL 3000 (PSI, Czech rep); The arrows in the color corresponding to lines indicate the time when NH_4Cl (final concentration of 0.7 mM) was added – start, 10%, 20%, 30% and 40% of protocol duration; the bars depict the different phases of protocol, the dark phase at the

end of the protocol leads to recovery of fluorescence quenching (for explanation of the protocol, refer to section 3.1 and 5.10, Figure 10).

6.5 Nonphotochemical fluorescence quenching *in vitro*

Antennae fractions isolated by sucrose gradient (pigment protein complexes F2, section 6.2) were used to study the mechanism of NPQ *in vitro*. The method was described previously (Kana et al., 2012; Ruban et al., 1994). The F2 fraction containing light harvesting antennae of *C. velia* (see Figure 15A) was diluted in a buffer without detergent of pH 7.6 (24 µl of antennae in 948 µl 10mM HEPES, 10 mM sodium citrate, pH 7.6) to test the role of protein aggregation in NPQ stimulation. Afterwards different amount of 5% HCl (see section 5.11) was added to decrease the pH (see Figure 28). The same amount of antennae fraction was diluted in the buffer of pH 5.5 (24 µl of antennae in 948 µl 10mM HEPES, 10 mM sodium citrate, pH 5.5) and the same protocol was performed. The fluorescence in pH 7.6 was higher than in buffer of pH 5.5, however, after acidifying the buffer of pH 7.6 to pH 5.5, the decrease in fluorescence was visible and it reached the same value as in the buffer with original pH 5.5. The reversibility of this process has been confirmed by *n*-Dodecyl β-D-maltoside addition (to the final concentration of 200 mM), which caused full recovery of initial fluorescence value (Fig. 28 and 29). This increase was not induced by a release of chlorophyll *a* from pigment-proteins, as controlled by kinetic measurements of fluorescence spectra (data not shown).

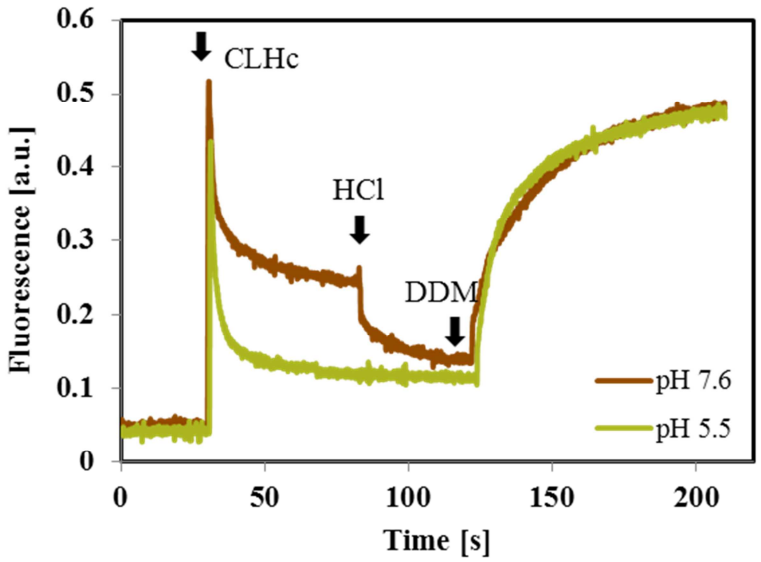

Figure 28: Effect of pH on NPQ in isolated CLHc of fraction F2 from sucrose gradient; green line represent the fluorescence of antennae diluted in the buffer with original pH of 5.5; brown line represents the antennae diluted in the buffer of pH 7.6, which was subsequently reduced by HCl to pH 5.5; Arrow CLHc represents the time when antennae fraction were added into the buffer, arrow HCl on the brown line represents the time when the pH was changed to 5.5 by HCl addition and arrow DDM represents the time when β-DDM was introduced into the cuvette to induce fluorescence recovery; the data were recorded by FL 100 (PSI Czech rep., see section 5.11)

In the second experiment, antennae fraction was diluted in the buffer (24 µl of antennae in 948 µl 10mM HEPES, 10 mM sodium citrate, pH 7.6) and the pH of the solution was stepwise reduced by adding HCl (see Figure 29). Quenching was observed already at the pH 7.6, but with lower pH, the quenching was higher. These results from titration experiment showed clear dependence of NPQ on pH, mimicking what happens *in vivo* during building up of light-induced ΔpH. The decrease in pH increased NPQ with saturation for pH of 4.5. The role of pH and aggregation was confirmed by these experiments.

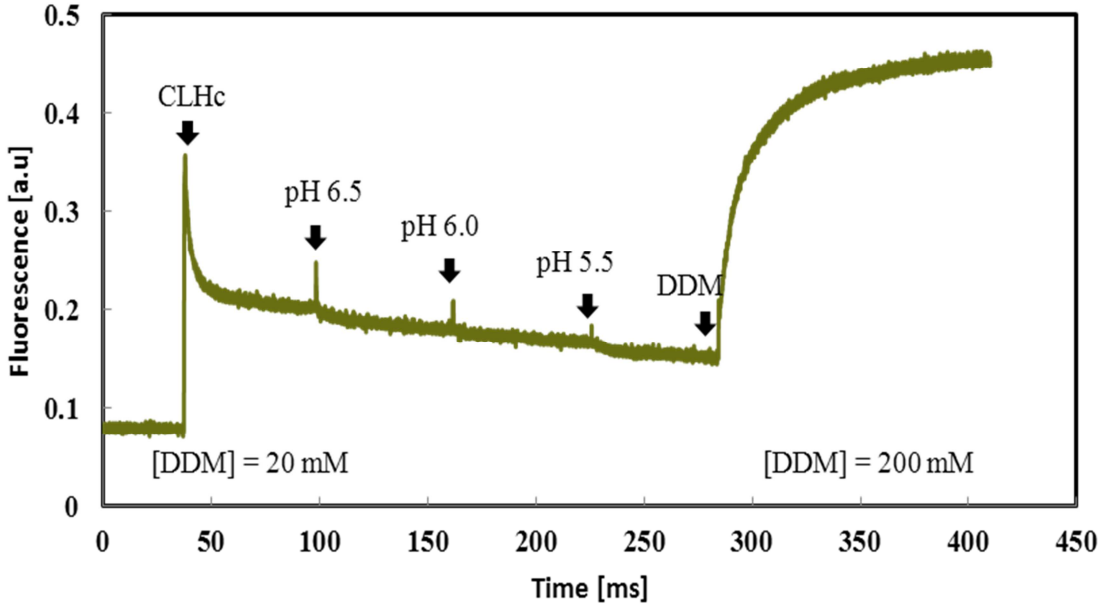

Figure 29: The analysis of NPQ of F2 from sucrose density gradient containing CLHc. Response to pH change and β-DDM addition was tested and chlorophyll a fluorescence was recorded by FL 100 (PSI Czech rep.) – see section 5.11, arrow with CLHc represents the time, when the antennae fraction F2 from sucrose gradient was added into the buffer, arrows with pH values represents time when corresponding amount of HCl (see section 5.11) was added into the reaction to reduce the pH to the value above the arrow (pH 6.5, 6.0 and 5.5), arrow with DDM represents the time when β-DDM was introduced into the cuvette to induce fluorescence recovery

7 Discussion

The main goal of this diploma thesis was isolation of native light harvesting complexes from thylakoid membranes in a selected strain and optimization of biochemical methods of their isolation. The ultimate goal was then characterization of nonphotochemical quenching in these isolated complexes (pH dependence and protein aggregation) in comparison with *in vivo* measurements. *C. velia* turned out to be a good model organism due to its unique features – it is evolutionary related to apicomplexan parasites and algae and it has a specific regulation of photosynthesis (Kotabova et al., 2011). Moreover its genome has been already sequenced and it will be soon fully accessible which will enable a complex research on antennae proteins and regulation of photosynthesis in this species.

The first task of this thesis was to ensure that *C. velia* cells are harvested in the exponential phase. We estimated specific growth rates of *C. velia* under continuous light regime (100 µmol m^{-2} s^{-1}) for three biological samples (see table I, section 6.1) We observed higher specific growth rates in first two biological samples (C.V.1 and C.V.2) than in the third sample (C.V.3). Generally, we observed faster growth rates in comparison to previous results (Foster et al., 2014; Quigg et al., 2012). Only in the "C.V.3" sample was $\mu = 0.34$ $days^{-1}$ comparable to the previous results of $\mu = 0.27$ $days^{-1}$ (Foster et al., 2014) (12:12 light-dark cycle and 165 µmol m^{-2} s^{-1}) and also to the result of $\mu = 0.37$ $days^{-1}$ (Quigg et al., 2012) (sinusoidal regime 12:12 light-dark cycle, max 500 µmol m^{-2} s^{-1}). The profile of "C.V.3" sample on the coulter counter (data not shown) revealed stacks of cells of bigger diameter then those in other two samples (C.V.1 and C.V.2), even though the samples were treated all the time the same and all of them were sonicated prior to analysis on coulter counter in order to separate the cells. Successful sonication could be an explanation for faster specific growth rates of our two samples (C.V.1 and C.V.2), because in these samples the cells were separated properly and that could be the reason for different results from other studies (Foster et al., 2014; Quigg et al., 2012) as we don't know how did they treated the cells prior to analysis. For further measurements the cells were always harvested on 4^{th} or 5^{th} day after dilution. For optimization of *C. veli*a growth we suggest sonication of the cells prior to analysis and also trial of modified buffered medium of basic artificial sea water with f/2 additives (Guillard and Ryther, 1962) and 25 mM HEPES which was successfully used for diatoms (Ewe, 2015).

The antennae proteins from the cell were isolated by sucrose density gradient centrifugation, the first isolation technique we tested. Solubilized *C. velia* thylakoid membranes (in 2% β-DDM) were loaded on the linear (5-20%) gradient of sucrose that showed mildly differentiated antennae bands (see Figure 15A). The technique was further optimized when a different concentrations of β-DDM were tested, however it did not improved the separation (data not shown). Therefore, the concentration of sucrose was refined to 5-15% in order to see borders in between the complexes. Unfortunately, even in this case it was not possible to separate the bands completely (see Figure 15B). Absorption spectra (section 6.2.1) and low temperature fluorescence spectra (section 6.2.2) showed different biophysical properties in between fractions F1 and F2. F1 contained higher amount of uncoupled pigments (mainly carotenoids) than F2 and they had different emission maximum. The pigment analysis by HPLC (section 6.2.3) of fractions F1 and F2 (Figure 15A) showed that F1 in comparison to F2 contained higher amount of violaxanthin, similar amount of isofucoxanthin and less amount of chlorophyll *a* in the ratio to the total pigments that is in line with our previous results (Kaňa et al., 2015).

Fractions F1 and F2 from sucrose gradient (Figure 15A) were used for measurements of absorbance spectra (section 6.2.1), low temperature fluorescence spectra (section 6.2.2), HPLC analysis (section 6.2.3) and also for measurements of NPQ on isolated antennae (section 6.6). Fractions F1 and F2 from sucrose gradient (Figure 15B) were for further characterization divided into more fractions (F1 into S1 and S2; F2 into S3, S4, S5) and studied by means of SDS-PAGE (see Figure 19). Fraction S1 from the sucrose gradient (see figure 19) did not contain proposed CLHc antenna proteins usually found in C. velia with molecular weight between 18 kDa and 20 kDa (Bina et al., 2014; Janouškovec et al., 2013; Quigg et al., 2012; Tichy et al., 2013). These proteins were present in fractions S3 and S5 (Figure 19). Fraction S1 contained larger proteins between 30 and 46 kDa which origin is not clear. Previous results could indicate that they possibly correspond to split psaA proteins of PSI (namely psaA-2) that is divided into 4-helix psaA1 and 7-helix conserved psaA-2 (Janouškovec et al., 2013). Fractions S3 and S5 had very similar composition containing previously mentioned antennae proteins of approx. 20 kDa. The protein pattern of antennae in our isolation (Figure 19) was similar to the one previously isolated from sucrose gradients (Mann et al., 2014), however the molecular masses of proteins in this study do not match with our data (although our data match with all the previously mentioned studies). As one could expect, fraction S6 (Figure 19) containing complexes of the highest molecular weight probably contains supercomplex of photosystems – PSI+PSII (Tichy et al., 2013). However,

there was nothing on the SDS-PAGE gel (Figure 19B) maybe due to little amount of the sample we loaded. Finally, fraction S7 contained a lot of proteins and some of the proteins even did not enter the gel (see nr.7 on Figure 19B). We can speculate that this fraction correspond to some insolubilized material or to some great complexes.

We confirmed that sucrose density gradient centrifugation can be successfully used for separation of *C. velia* antennae complexes in line with previous results (Kaňa et al., 2015; Tichy et al., 2013). In the previous work (Tichy et al., 2013) the continual sucrose concentration of 0-1.0M was used, where proper separation of PSI and PSII from antennae complexes was achieved but antennae bands were not separated well in line with our results (Figure 15). In this study, higher concentration of β – DDM (5% per 1 mg of Chl) was used (compared to our 2% or 1% β – DDM), which better fits for solubilization of bigger complexes (PSI+PSII) in greater amount. The sucrose density gradient centrifugation is commonly used for separation of higher plants antennae proteins and complexes (Caffarri et al., 2009). The method was also used for isolation of antennae proteins of alga *Rhodomonas salina* (Kana et al., 2012), thylakoid proteins of cyanobacterium *Synechocystis* PCC 6803 (Daddy et al., 2015) and in diatoms (Buchel, 2003), where different oligomeric states of antennae where observed on the contrary with our results. The method of sucrose density gradient centrifugation for separation of *C. velia* complexes was not suitable for obtaining pure antennae proteins and it needs to be followed by other purification steps – e.g. ion exchange chromatography or gel filtration (Bina et al., 2014).

To improve antennae separation, the isoelectric focusing (IEF) was tested. This technique has been successfully used for isolation of the proteins from *Spinacia oleracea* (Ruban et al., 1994), Arabidopsis thaliana (Behrens et al., 2013; Moffatt et al., 1991) and *Zea mays* (Bassi and Dainese, 1992). The IEF gel (Figure 20) displayed two groups of proteins containing further sub-bands: the first group I (pI of 4-4.25) differentiated into four sub-bands and the second group II (pI around 5) into two bands. However the separation inside of those two groups (I and II) was not proper due to insufficient amount of solubilized thylakoid membranes used for this technique. From that reason the bands are poorly visible on the photo (Figure 20). As we did not have enough material to follow the typical protocol (when IEF bands are usually cleaned by gel chromatography), the absorption spectra (not shown) and low temperature fluorescence spectra (section 6.3.1) were affected by presence of ampholytes. Low temperature fluorescence spectra (Figure 21) had shifted maxima of 678 and 677 nm in comparison to spectra of fractions from sucrose gradient (Figure 17), which could be caused by presence of ampholytes.

Protein composition of IEF bands was analyzed by polyacrylamide gel electrophoresis followed by silver staining, because the concentrations of the proteins were too low. We obtained relatively good separation showing different protein content in particular IEF fractions (Figure 22). All fractions from the first group (Figure 20) contained different pattern of supposedly antennae proteins (18-30 kDa), we were concentrated mostly on possible antennae proteins in between 18-25 kDa. Fraction I1 was different from fractions I2-I4 and contained a doublet (between 18-20 kDa). Fraction I2 contained a 20 kDa protein similar to the antenna complex from F2 (S3 and S5) of sucrose gradient (see Figure 19). Fraction I3 and I4 were both enriched in antennae proteins of approx. 20 kDa, however there was a lower molecular weight band present in fractions I4 and maybe also I5 and I6 (see Figure 22). The pI of the first group is similar to pI of LHCII isolated from higher plants – *zea mays* with LHCII pI of 4.24, 4.28 and 4.33 (Bassi and Dainese, 1992) or Arabidopsis thaliana with LHCII pI of 4.00, 4.05 and 4.10 (Jackowski et al., 2000). The pI (around 5) of the second group II (see Figure 20) corresponds to the pI of PSII reaction center complex (Jackowski et al., 2000).

Technique of isoelectric focusing was found to be suitable for isolation of light harvesting proteins, however for our purpose it needs to be optimized. Firstly, more material is needed to be loaded on the gel. Secondly, less concentration of the detergent is needed throughout the gel – I would recommend 0.04 % (successfully used for sucrose gradient centrifugation) instead of 0.06 %. Moreover it would help to use a narrower pH window of ampholytes – e.g. pH 3-4.5 instead of pH 2.5 – 5 in order to obtain better separation.

The third method we have tested for isolation of antennae proteins form *C. velia* was anion exchange chromatography (see section 5.5). This technique seems to be promising, because it is fast and relatively easy to handle in comparison to sucrose gradients and isoelectric focusing. The resulting chromatogram (Figure 23) showed a separation of thylakoid membrane proteins into four fractions E1-E4. Fraction E1 and E2 were properly separated from fractions E3 and E4, whereas E3 and E4 formed a double peak. The absorbance spectra (Figure 24) of fraction E1 showed chlorophyll maximum of 673 nm, but fractions E2-4 had almost the same spectra with the chlorophyll maximum of 678 nm. Similarly, in low temperature fluorescence spectra (Figure 25) – fraction E1 peaking at 679 nm differed from fractions E2-4 with the maximum of 685 nm. This fraction was enriched in free pigments similarly to the F1 from sucrose gradient (see Figure 25B and Figure 17). Red-shifted spectra indicated that this method yielded the most intact sample.

Anion exchange chromatography was successfully used for isolation of *C. Velia* proteins (Bina et al., 2014; Tichy et al., 2013) or for purification of extracellular phenol oxidase from *Tetracystis aeria* (Otto and Schlosser, 2014). The best results were obtained when IEC is coupled to gel chromatography. However, we still need to optimize the proper detergent concentration in order to solubilize all the antennae complexes from thylakoid membrane. Therefore, for future experiments I would propose to try affinity chromatography with immobilized *C. velia* thylakoid membranes and linear gradient of β – DDM in mobile phase, in order to clearly see in which concentration of β – DDM are certain complexes solubilized. Moreover we should try to optimize the anion gradient during the procedure to obtain proper separation also in between the fractions E3 and E4.

Nonphotochemical quenching was measured on the whole cells of *C. velia*. Orange light induced NPQ leading to fast decrease in fluorescence as already observed in other studies (Kotabova et al., 2011; Mann et al., 2014). *C. velia* is able to develop higher NPQ value e.g. in comparison to *P. tricornutum* (Schumann et al., 2007) and it exhibits fast fluorescence quenching followed by slow recovery in the dark (see Figure 26). The role of pH on the fluorescence quenching *in vivo* was tested by addition of uncoupler of fluorescence quenching – NH_4Cl (see section 6.5). Analysis of NPQ on intact *C. velia* cells after uncoupler addition has showed different relaxation kinetics in comparison to higher plants (Ruban et al., 2004). The uncoupler was introduced to the cells during a different period of the protocol. When it was added before the period light, no NPQ was observed and fluorescence stayed the same. When it was added during the light illumination, *C. velia* was locked in NPQ state in contrast to intact spinach chloroplasts with immediate response to uncoupler (NH_4Cl). The situation in diatoms (*P. tricornutum*) is somewhere in between the response of higher plants and *C. velia* which is supposed to be caused by the fact, that NH_4Cl accelerates not only the reversibility of NPQ but also the rate of epoxidation of xanthophylls (Ruban et al., 2004).

We have tested three methods for antennae isolation, however only sucrose gradient provided us with enough material of relatively-well characterized antennae proteins for further measurements of NPQ. Role of pH and possible CLHc aggregation was then studied *in vitro on* isolated CLHc (F2 from sucrose gradient – see Figure 15). *In vitro* quenching showed dependence of NPQ on pH and CLHc aggregation – the lower was the pH, the higher was the NPQ. This process was fully reversible – fast fluorescence recovery was observed after addition of β – DDM into the reaction, displaying similar behavior to that of isolated antenna from higher plants. However, in order to study only the effect of pH, we

need to refine the initial concentration of detergent at the beginning of the experiment. I would suggest following the procedure already described for recombinant apoproteins from E. coli mixed with pigments (Belgio et al., 2014) where 0.003% β – DDM was used to study the effect of pH.

We have identified nonphotochemical quenching in CLH antennae which is dependent on the pH and aggregation. These data are important for further characterization and determination of NPQ locus in CLH antennae. The great advantage for this project is already sequenced genome of *C. velia* which will be soon accessible. It is already known that *C. velia* has many antennae genes - twenty three LHC homologs obtained from *C. velia* were aligned with other algal species giving the result of phylogenetic relationships with diatoms, brown algae, dinoflagellates, green algae, chromalveolates red algae (Pan et al., 2012). For further study we would like to test which antennae genes are expressed under which conditions and we would like to determine the locus of NPQ. Further goals are: to study of zeaxanthin role in NPQ and isolation of pure antennae to make further NPQ experiments *in vitro* and possibly in proteoliposomes.

8 Conclusion

Chromera velia Light Harvesting Antennae (CLH) were isolated by three different methods, by sucrose density centrifugation, isoelectric focusing and by anion exchange chromatography. These methods were further optimized and isolated CLHc were characterized spectroscopically by means of low temperature fluorescence spectroscopy and by absorbance spectroscopy. Pigment composition was described by high performance liquid chromatography and proteins content by polyacrylamide gel electrophoresis. The results were compared to previous studies and our data have shown expected protein and pigment composition. The proper biochemical isolation allowed us to explore a unique mechanism of nonphotochemical quenching in this species on antennae level. We have studied role of pH and CLH aggregation that both were identified to be crucial. These experiments enable future study of NPQ locus in CLH antennae, function of CLH antennae in light-harvesting, and construction of model of photoprotective nonphotochemical quenching in *C. velia*.

9 References

Alboresi, A., Gerotto, C., Giacometti, G. M., Bassi, R., and Morosinotto, T. (2010). *Physcomitrella patens* mutants affected on heat dissipation clarify the evolution of photoprotection mechanisms upon land colonization. *Proceedings of the National Academy of Sciences of the United States of America* **107**, 11128-11133.

Allen, J. (1995). Thylakoid Protein - Phosphorylation, State-1-State-2 Transitions, and Photosystem Stoichiometry Adjustment - Redox Control at Multiple Levels of Gene-Expression. *Physiological Plantarum* **93**, 196-205.

Bassi, R., and Dainese, P. (1992). A Supramolecular Light-Harvesting Complex from Chloroplast Photosystem-II Membranes. *European Journal of Biochemistry* **204**, 317-326.

Behrens, C., Hartmann, K., Sunderhaus, S., Braun, H. P., and Eubel, H. (2013). Approximate calculation and experimental derivation of native isoelectric points of membrane protein complexes of Arabidopsis chloroplasts and mitochondria. *Biochimica et Biophysica Acta* **1828**, 1036-46.

Belgio, E., Kapitonova, E., Chmeliov, J., Duffy, C. D. P., Ungerer, P., Valkunas, V., and Ruban, A. V. (2014). Economic photoprotection in photosystem II that retains a complete light-harvesting system with slow energy traps. *Nature Communications* **5**.

Bina, D., Gardian, Z., Herbstova, M., Kotabova, E., Konik, P., Litvin, R., Prasil, O., Tichy, J., and Vacha, F. (2014). Novel type of red-shifted chlorophyll a antenna complex from *Chromera velia*: II. Biochemistry and spectroscopy. *Biochimica et Biophysica Acta* **1837**, 802-10.

Brown, B., Ambarsari, I., Warner, M., Fitt, W., Dunne, R., Gibb, S., and Cummings, D. (1999). Diurnal changes in photochemical efficiency and xanthophyll concentrations in shallow water reef corals: evidence for photoinhibition and photoprotection. *Coral Reefs* **18**, 99-105.

Buchel, C. (2003). Fucoxanthin-chlorophyll proteins in diatoms: 18 and 19 kDa subunits assemble into different oligomeric states. *Biochemistry* **42**, 13027-13034.

Buchel, C. (2015). Evolution and function of light harvesting proteins. *Journal of Plant Physiology* **172C**, 62-75.

Bungard, R., Ruban, A., Hibberd, J., Press, M., Horton, P., and Scholes, J. (1999). Unusual carotenoid composition and a new type of xanthophyll cycle in plants. *Proceedings of the National Academy of Sciences of the United States of America* **96**, 1135-1139.

Caffarri, S., Kouril, R., Kereiche, S., Boekema, E. J., and Croce, R. (2009). Functional architecture of higher plant photosystem II supercomplexes. *EMBO J* **28**, 3052-63.

Carbonera, D., Gerotto, C., Posocco, B., Giacometti, G. M., and Morosinotto, T. (2012). NPQ activation reduces chlorophyll triplet state formation in the moss *Physcomitrella patens*. *Biochimica et Biophysica Acta* **1817**, 1608-15.

Cavalier-Smith, T. (1999). Principles of protein and lipid targeting in secondary symbiogenesis: Euglenoid, dinoflagellate, and sporozoan plastid origins and the eukaryote family tree. *Journal of Eukaryotic Microbiology* **46**, 347-366.

Cumbo, V. R., Baird, A. H., Moore, R. B., Negri, A. P., Neilan, B. A., Salih, A., van Oppen, M. J., Wang, Y., and Marquis, C. P. (2013). *Chromera velia* is endosymbiotic in larvae of the reef corals *Acropora digitifera* and *A. tenuis*. *Protist* **164**, 237-44.

Daddy, S., Zhan, J., Jantaro, S., He, C., He, Q., and Wang, Q. (2015). A novel high light-inducible carotenoid-binding protein complex in the thylakoid membranes of *Synechocystis* PCC 6803. *Scientific Reports* **5**, 9480.

Demmig-Adams, B. (1990). Carotenoids and photoprotection in plants: A role for the xanthophyll zeaxanthin. *Biochimica et Biophysica Acta - Bioenergetics* **1020**, 1–24.

Dimier, C., Giovanni, S., Ferdinando, T., and Brunet, C. (2009). Comparative ecophysiology of the xanthophyll cycle in six marine phytoplanktonic species. *Protist* **160**, 397-411.

Engelken, J., Brinkmann, H., and Adamska, I. (2010). Taxonomic distribution and origins of the extended LHC (light-harvesting complex) antenna protein superfamily. *BMC Evolutionary Biology* **10**.

Ewe, D. (2015). Living well with a scrambled metabolism: CO_2 fixation and carbohydrate pathways in the diatom *Phaeodactylum tricornutum*. PhD. thesis, Universität Konstanz.

Foster, C., Portman, N., Chen, M., and Slapeta, J. (2014). Increased growth and pigment content of *Chromera velia* in mixotrophic culture. *FEMS Microbiology Ecology* **88**, 121-8.

Gilmore, A. (1997). Mechanistic aspects of xanthophyll cycle-dependent photoprotection in higher plant chloroplasts and leaves. *Physiological Plantarum* **99**, A88

Goss, R., and Lepetit, B. (2014). Biodiversity of NPQ. *Journal of Plant Physiology*.

Goss, R., Quaas, T., Berteotti, S., Ballottari, M., Flieger, K., Bassi, R., and Wilhelm, C. (2015). Non-photochemical quenching and xanthophyll cycle activities in six green algal species suggest mechanistic differences in the process of excess energy dissipation. *Journal of Plant Physiology* **172**, 92-103.

Green, B., and Pichersky, E. (1994). Hypothesis for the evolution of three-helix Chl a/b and Chl a/c light-harvesting antenna proteins from two-helix and four-helix ancestors. *Photosynthesis Research* **39**, 149-162.

Guillard, R. R., and Ryther, J. H. (1962). Studies of marine planktonic diatoms I. *Cyclotella nana Hustedt* and *Detonula confervacea* (cleve) gran. *Canadian Journal of Microbiology* **8**, 229-239.

Gunning, B. a. S., OM (1999). Confocal microscopy of thylakoid autofluorescence in relation to origin of grana and phylogeny in the green algae. *Australian Journal of Plant Physiology* **26**, 695-708.

Horton, P., Ruban, A. V., and Walters, R. (1996). Regulation of light harvesting in green plants. Vol. 47, pp. 655-684, Annual Review of Plant Physiology and Plant Molecular Biology

Jackowski, G., Kacprzak, K., and Jansson, S. (2000). Identification of Lhcb1/Lhcb2/Lhcb3 heterotrimers of the main lightharvesting chlorophyll a/b-protein complex of Photosystem II (LHC II). *Biochimica et Biophysica Acta* **1504**, 340-345.

Janouskovec, J., Horak, A., Obornik, M., Lukes, J., and Keeling, P. J. (2010). A common red algal origin of the apicomplexan, dinoflagellate, and heterokont plastids. *Proceedings of the National Academy of Sciences of the United States of America* **107**, 10949-54.

Janouškovec, J., Sobotka, R., Lai, D.-H., Flegontov, P., Koník, P., Komenda, J., Ali, S., Prášil, O., Pain, A., Oborník, M., Lukeš, J., and Keeling, P. J. (2013). Split Photosystem

Protein, Linear-Mapping Topology, and Growth of Structural Complexity in the Plastid Genome of *Chromera velia*. *Molecular Biology and Evolution* **30**, 2447-2462.

Jeffrey, S., and Vesk, M. (1997). Introduction to marine phytoplankton and their pigment signatures. *Phytoplankton pigments in oceanography* **37-84**.

Kaňa, R., Kotabová, E., Kopečná, J., Trsková, E., Belgio, E., Sobotka, R., and Ruban, A. V. (2015). Violaxanthin inhibits nonphotochemical quenching in light-harvesting antennae of *Chromera velia*. *FEBS Letters* **submitted**.

Kana, R., Kotabova, E., Sobotka, R., and Prasil, O. (2012). Non-photochemical quenching in cryptophyte alga *Rhodomonas salina* is located in chlorophyll a/c antennae. *PLoS One* **7**, e29700.

Karp, G. (2010). Cell and Molecular Biology. *In* "Concepts and experiments" (K. Witt, ed.). John Wiley & Sons, Inc, USA.

Keeling, P. J. (2013). The Number, Speed, and Impact of Plastid Endosymbioses in Eukaryotic Evolution. *Annual Review of Plant Biology* **64**, 583-607.

Koolman, J., and Roehm, K.-H. (2005). "Color Atlas of Biochemistry," 2nd/Ed. Thieme New York, Germany, USA.

Kotabova, E., Kana, R., Jaresova, J., and Prasil, O. (2011). Non-photochemical fluorescence quenching in *Chromera velia* is enabled by fast violaxanthin de-epoxidation. *FEBS Letters* **585**, 1941-5.

Lavaud, J., Rousseau, B., and Etienne, A. (2002). In diatoms, a transthylakoid proton gradient alone is not sufficient to induce a non-photochemical fluorescence quenching. *FEBS Letter* **523**, 163-166.

Li, X., Bjorkman, O., Shih, C., Grossman, A., Rosenquist, M., Jansson, S., and Niyogi, K. (2000). A pigment-binding protein essential for regulation of photosynthetic light harvesting. *Nature* **403**, 391-395.

Lohr, M. a. W., C (1999). Algae displaying the diadinoxanthin cycle also possess the violaxanthin cycle. *Proceedins of the National Academy of Sciences of the United States of America* **96** 8784-8789.

MacIntyre, H., Kana, T., and Geider, R. (2000). The effect of water motion on short-term rates of photosynthesis by marine phytoplankton. *Trends in Plant Science*.

Mann, M., Hoppenz, P., Jakob, T., Weisheit, W., Mittag, M., Wilhelm, C., and Goss, R. (2014). Unusual features of the high light acclimation of *Chromera velia*. *Photosynthesis Research*.

Moffatt, B., Pethe, C., and Laloue, M. (1991). Metabolism of Benzyladenine is Impaired in a Mutant of *Arabidopsis thaliana* Lacking Adenine Phosphoribosyltransferase Activity. *Plant Physiology* **95**, 900-908.

Moore, R. B., Obornik, M., Janouskovec, J., Chrudimsky, T., Vancova, M., Green, D. H., Wright, S. W., Davies, N. W., Bolch, C. J., Heimann, K., Slapeta, J., Hoegh-Guldberg, O., Logsdon, J. M., and Carter, D. A. (2008). A photosynthetic alveolate closely related to apicomplexan parasites. *Nature* **451**, 959-63.

Neilson, J. A., and Durnford, D. G. (2010). Structural and functional diversification of the light-harvesting complexes in photosynthetic eukaryotes. *Photosynthesis Research* **106**, 57-71.

Niyogi, K. K., Muller, P., and Li, X.-P. (2001). Non-Photochemical Quenching. A Response to Excess Light Energy. *Plant Physiology* **125**.

Obornik, M., Vancova, M., Lai, D. H., Janouskovec, J., Keeling, P. J., and Lukes, J. (2011). Morphology and ultrastructure of multiple life cycle stages of the photosynthetic relative of apicomplexa, *Chromera velia*. *Protist* **162**, 115-30.

Otto, B., and Schlosser, D. (2014). First laccase in green algae: purification and characterization of an extracellular phenol oxidase from *Tetracystis aeria*. *Planta* **240**, 1225-36.

Pan, H., Slapeta, J., Carter, D., and Chen, M. (2012). Phylogenetic analysis of the light-harvesting system in *Chromera velia*. *Photosynthesis Research* **111**, 19-28.

Pan, X., Li, M., Wan, T., Wang, L., Jia, C., Hou, Z., Zhao, X., Zhang, J., and Chang, W. (2011). Structural insights into energy regulation of light-harvesting complex CP29 from spinach. *Nature Structural & Molecular Biology* **18**, 309-15.

Pinnola, A., Dall'Osto, L., Gerotto, C., Morosinotto, T., Bassi, R., and Alboresi, A. (2013). Zeaxanthin binds to light-harvesting complex stress-related protein to enhance nonphotochemical quenching in *Physcomitrella patens*. *Plant Cell* **25**, 3519-34.

Pogson, B. R., HM (2000). Genetic manipulation of carotenoid biosynthesis and photoprotection. *Philosophical Transactions of the Royal Society of London Series B - Biological Sciences* **355**, 1395-1403.

Quigg, A., Kotabova, E., Jaresova, J., Kana, R., Setlik, J., Sediva, B., Komarek, O., and Prasil, O. (2012). Photosynthesis in *Chromera velia* represents a simple system with high efficiency. *PLoS One* **7**, e47036.

Ruban, A. (2013). "The Photosynthetic Membrane," John Wiley & Sons, Ltd., United Kingdom.

Ruban, A., Lavaud, J., Rousseau, B., Guglielmi, G., Horton, P., and Etienne, A. (2004). The super-excess energy dissipation in diatom algae: comparative analysis with higher plants. *Photosynthesis Research* **82**, 165-175.

Ruban, A., Walters, R., and Horton, P. (1992). The Molecular Mechanism of the Control of Excitation-Energy Dissipation in Chloroplast Membranes - Inhibition of Delta-pH-dependent Quenching of Chlorophyll Fluorescence by Dicyclohexylcarbodiimide. *Febs Letters* **309**, 175-179.

Ruban, A. V., Young, A. J., Pascal, A. A., and Horton, P. (1994). The Effects of lllumination on the Xanthophyll Composition of the Photosystem II Light-Harvesting Complexes of Spinach Thylakoid Membranes. *Plant Physiology* **104**, 227-234.

Schumann, A., Goss, R., Torsten, J., and Wilhelm, C. (2007). Investigation of the quenching efficiency of diatoxanthin in cells of *Phaeodactylum tricornutum* (Bacillariophyceae) with different pool sizes of xanthophyll cycle pigments. *Phycologia* **46**, 113-117.

Tanabe, Y., Shitara, T., Kashino, Y., Hara, Y., and Kudoh, S. (2011). Utilizing the Effective Xanthophyll Cycle for Blooming of *Ochromonas smithii* and *O. itoi* (Chrysophyceae) on the Snow Surface. *PLoS One* **6**.

Tichy, J., Gardian, Z., Bina, D., Konik, P., Litvin, R., Herbstova, M., Pain, A., and Vacha, F. (2013). Light harvesting complexes of *Chromera velia*, photosynthetic relative of apicomplexan parasites. *Biochimica et Biophysica Acta* **1827**, 723-9.

van Amerongen, H., Chukhutsina, V. U., and Buchel, C. (2014). Disentangling two non-photochemical quenching processes in Cyclotella meneghiniana by spectrally-resolved picosecond fluorescence at 77K. *Biochimica et Biophysica Acta* **1837**, 899-907.

Wolfe, G. R., Cunningham, F. X., Durnfordt, D., Green, B. R., and Gantt, E. (1994). Evidence for a common origin of chloroplasts with light-harvesting complexes of different pigmentation. *Nature* **367**, 566-568.

Yamamoto, H., Chichester, C., and Nakayama, T. (1962). Studies on Light and Dark Interconversions of Leaf Xanthophylls. *Archives of Biochemistry and Biophysics* **97**.

Zhang, Z., Shrager, J., Jain, M., Chang, C. W., Vallon, O., and Grossman, A. R. (2004). Insights into the survival of *Chlamydomonas reinhardtii* during sulfur starvation based on microarray analysis of gene expression. *Eukaryotic Cell* **3**, 1331-48.